UNIVERSIDADE
BEIRA INTERIOR

Experimental and Numerical Analysis of a Sprint Canoe for the Olympic Games
Versão corrigida após defesa da dissertação

João Pedro Pereira Amorim

Dissertação para obtenção do Grau de Mestre em
Engenharia Aeronáutica
(Mestrado Integrado)

Orientador: Prof. Doutor André Resende Rodrigues da Silva
Co-orientadora: Prof. Doutora Beatriz Branquinho Gomes

março de 2021

Dedication

To my parents.

Acknowledgements

Throughout my dissertation and academic journey there were many important people to whom I want to thank.

First of all, my parents, for making all this possible, for always believing in me, for always supporting me in everything and for always giving me access to the best education. In the same way, I want to thank my remaining family and friends who accompanied me during this journey, also being a fundamental pillar of my life and for supporting me in good and bad moments.

During the realization of this dissertation I also had support that were fundamental and to whom I am very grateful, first of all to my supervisor Prof. André Resende Rodrigues da Silva, for accepting this project with open arms and guiding me throughout this journey and to Prof. Dr. Beatriz Branquinho Gomes for being readily available to be part of the project and giving essential help to the realization of the same. In the same way, I would like to thank AEROG for having been great companions, a special thanks to Daniel Vasconcelos and Emanuel Camacho, PhD students.

At the same time, I would like to thank NELO M.A.R. Kayaks for believing in me and giving me this opportunity to do more for canoeing, as they have done over the last years helping Portuguese canoeing to grow more and more. A special greeting to Nuno Ramos and André Santos for all their availability. Last but not least, I would like to thank the Portuguese canoeing family for all the help and support throughout this project, namely Marco, Bruno and César for accepting to participate and for lending their training equipment, Vitor Cruz, Duarte Lacerda, Clube Náutico de Ponte de Lima and all the others that always made themselves available to help.

Finally, I would like to thank the Montemor-o-velho City Hall and the CAR de Montemor-o-velho for the easy access to their facilities to carry out the experimental tests.

Resumo

A cultura portuguesa esteve sempre interligada com a cultura náutica. Atualmente, Portugal é uma potência na modalidade de canoagem. Para além de atletas, excelentes locais de treino, Portugal, é um dos melhores fabricantes de canoas e kayaks a nível mundial. Para haver uma constante evolução dos designs dos barco, é crucial estudar a hidrodinâmica das canoas. Assim, este trabalho surge no âmbito da falta de estudos científicos na área da hidrodinâmica na canoagem, principalmente da embarcação C1.

Nesta dissertação foram realizadas simulações de Dinâmica de Fluidos Computacional (*CFD*), com o objetivo de simular o escoamento de água e ar em torno do casco de duas canoas, para avaliar a performance destas. Para isso, foi utilizado o método do Volume de Fluido (*VoF*) para simular a superfície livre, e o modelo de turbulência κ-ε Standard para simular a turbulência. Foi também realizado um estudo de independência de malha para garantir que a malha utilizada não afeta os resultados pretendidos. O *software* utilizado para esta análise foi o Ansys Fluent 2019 R3.

Com vista a validar o estudo numérico, foram realizados testes experimentais à escala real. O modelo numérico foi então aplicado às duas embarcações, onde foi estudada a resistência ao avanço das canoas para uma gama de velocidades, assim como para diferentes arfagens.

Também para efeitos de comparação foram avaliadas a elevação de onda, assim como o efeito da canoa nas velocidades do escoamento em ambas as canoas.

Para o modelo C1 5 L, os valores foram sobrestimados numericamente, enquanto que para o outro modelo, a C1 8 L, os resultados foram mais próximo dos valores obtidos experimentalmente. Outros estudos numéricos demonstraram problemas semelhantes, o que possivelmente terá a ver com a determinação exata da posição da linha de água, que influencia significativamente os resultados finais.

Palavras-chave

Canoagem, Hidrodinâmica, Design do casco, Experimental, Numérico, Resistência ao avanço

Abstract

Portuguese culture has always been interconnected with nautical culture. Nowadays, Portugal is a powerful country in canoeing. Besides athletes, excellent training places, Portugal is one of the best manufacturers of canoes and kayaks in the world. To have a constant evolution in the design of the boats, it is crucial to study the hydrodynamics of canoes. Therefore, the present work arises in the context of the lack of scientific studies in the area of hydrodynamics in canoeing, mainly the C1 boat.

In this dissertation, simulations of Computational Fluid Dynamics (*CFD*) were performed in order to simulate the water and air flow around the hull of two canoes to evaluate their performance. For this, the Fluid Volume method (*VoF*) was used to simulate the free surface, and the turbulence model κ-ε Standard to simulate the turbulence. A mesh independence study was also carried out to ensure that the mesh used does not affect the intended results. The *software* used for this analysis was Ansys Fluent 2019 R3.

In order to validate the numerical study, experimental tests were performed at full scale. The numerical model was then applied to the two vessels, where the resistance to advance of the canoes, at a range of velocities was studied, as well as for different pitch angle.

Also for comparison purposes the wave elevation, as well as the effect of the flow velocity, in both canoes were evaluated.

For the C1 5 L model, the values were overestimated numerically, while for the other model, the C1 8 L, the results were closer to the values obtained experimentally. Other numerical studies have shown similar problems, which possibly has to do with the exact determination of the waterline position, which significantly influences the final results.

Keywords

Canoeing, Hydrodynamics, Hull Design, Experimental, Numerical, Drag

Contents

List of Figures

List of Tables

List of Acronyms

AEROG	Aeronautics and Astronautics Research Center
CFD	Computational Fluid Dynamics
DES	Detached Eddy Simulation
DNS	Direct Numerical Simulations
FES	Institute for Research and Development of Sport Equipment
ICF	International Canoe Federation
LES	Large Eddy Simulation
PRESTO!	Pressure Staggering Option
RANS	Reynolds-averaged Navier-Stokes equations
UBI	Universidade da Beira Interior
VoF	Volume of Fluid
VWS	Versuchsanstalt für Wasserbau und Schiffbau

Nomenclature

$\dot{m}$ Mass flow

A_a Aerodynamical Frontal Area

A_{wet} Wetted Area

C_f Friction Coefficient

C_w Residual Drag Coefficient

D_a Aerodynamic Resistance

D_f Friction Drag

D_T Total Resistance

D_w Residual Wave Drag

g Gravitational Constant

U_H Hull Velocity

C Canoe

Fr Froude Number

G Generation of Turbulent Kinetic Energy

I Impulse

K Kayak

L Waterline Length

p Static Pressure

Re Reynolds Number

S Source Term

V Volume

Greek Symbols

Δ Displacement

ε Turbulent Dissipation Rate

κ Turbulent Kinetic Energy

μ Dynamic Viscosity

μ^+ Friction Velocity

ν Kinematic Viscosity

ϕ Other scalar Quantities

ρ Density

τ_w Shear Stress

y^+ Dimensionless Wall Distance

Chapter 1

Introduction

In this first chapter of this dissertation, a general introduction to the work will be given. This first section focuses on the motivation for this work, talking about a general context of the theme. In a second section, the objectives proposed for this dissertation are presented. Finally, in the last section, the structure of this dissertation that will be followed is presented.

1.1 Motivation

Nautical science has always had a strong emphasis on Portuguese culture and history and often worked as a lever in the search for knowledge and engineering methods. Since the Portuguese era of discoveries, numerous nautical innovations have been created or perfected by the Portuguese such as the caravel, the triangular sail, the astronomical navigation, the astrolabe, the quadrant, Jacob's staff, like many other instruments and methods used to sail in the open sea. Throughout history, the Portuguese were always at the forefront of maritime transport and nautical science [1].

Nowadays, Portugal has been becoming a world canoeing power country with some of the best world athletes and the best training centres due to the excellent conditions in our rivers and lakes for the practice of this sport. In addition to all these aspects, the current world leader in sprint kayak production, the Nelo M.A.R. Kayaks, is based in Portugal, Vila do Conde, being behind 27 of the 35 possible Olympic medals in the Rio de Janeiro edition of the Olympic Games in 2016. Factors like these boost a whole economy around industry, hotels, sports tourism that are important for the country, including some inland areas, that are sought for countless athletes, especially during the low winter season. It is also interesting to help our athletes achieve better results for our country. Through scientific knowledge applied to the sport.

The study of the hydrodynamic of the canoes is still very experimental, with very few published studies regarding numerical simulation to improve the canoe design, and the few that exist are related to kayak with very little or nothing related to the canoe boat. As an example, in Germany, some athletes have their personalised boats, studied in proper towing-tanks combined with numerical simulations at the Institute for Research and Development of Sports Equipment, also known by its German acronym, FES, which is behind many sports engineering innovations. As a result of this, no other country team has won more medals in the rowing, canoeing, and kayaking events than the German teams [2].

Joining my scientific knowledge acquired throughout the course, with my empirical knowledge as an athlete, in this dissertation, I will try to help Portuguese canoeing to continue at the forefront of nautical knowledge.

1.2 Objectives

The main goal of this work is to study a high-performance canoe, the C1 8 L, made by Nelo M.A.R. Kayaks that will participate in the 2021 Olympic Games in Tokyo, and compare it with the previous model, the Nelo C1 5 L, that has been used by some athletes in 2016 Olympic Games edition in Rio de Janeiro.

To carry out this study, a Computational Fluid Dynamics study will be held, using Ansys Fluent 2019 R3 software, and also experimental tests, in order to validate the numerical model. Through the numerical model, it will be possible to simulate many cases, which will help to better understand the performance of these vessels in competitive situation. For this, it will be simulated an incompressible and isothermal two-phase flow, with a steady approach assumption. The cases will be simulated to analyse the behaviour of these vessels at different velocities, which canoes reach in competition.

During the paddle stroke, the athlete varies his centre of mass, thus changing the attitude of the boat towards the flow since that may have zero, positive or negative angle of attack depending on the stroke phase. This work will also study the variation of the pitch angle, to find the angle that causes the canoe to produce less drag, helping the athlete find the best position in the canoe to get the best results.

Despite the unsteadiness of canoe motion due to the interaction between the canoe with the water free surface and interaction between the paddle blade and the hull flow, a steady-state approach will be used. It is assumed that the boat remains in a static position, without the presence of the athlete, and his movements, with the sole purpose of studying the hydrodynamics of the hull, a steady approach is a good approximation, with less computational cost when compared with transient simulation.

This work is a first step to optimise the canoe hull geometry in order to minimise drag and improve the boat performance.

1.3 Structure

This dissertation is organised as follows: Introduction, State-of-the-art, Experimental Study, Mathematical Model, Results and Discussion, Conclusions and Future Work.

This introduction chapter, is a brief description and presentation of the project, it is presented the motivation to do this work and also the goals to achieve in this dissertation.

In Chapter 2, a brief description of the sport is made, such as construction rules applied and a resumed the design evolution of these vessels. It is also carried a review of fluid mechanics concepts related to the movement and drag calculations related to marine vessels, more specifically canoes.

At Chapter 3, the method and procedure of the experimental tests made in this project are explained.

In Chapter 4, a general description of the governing equations of the flow used in the numerical simulation, such as multiphase flow and turbulence modelling are made. Following this, the details of the numerical procedure used in the simulations are described.

When all the simulations and tests are done, in the Chapter 5, it is presented and analysed the numerical results, and also faced with the experimental results obtained.

Finally, at Chapter 6, the conclusions reached during this dissertation, and also outlined possible future works that can be done following this work, are presented.

Chapter 2

State-of-the-art

In this chapter, in the opening sections, it will be presented an introduction to the sport, as well as the construction rules for canoes, according to International Canoe Federation. In the following sections, it will be reviewed some parameters of the canoe design, as well as the evolution through history, and finally, some hull drag principles. Finally, in the last section, a brief introduction to Computational Fluid Dynamics is made, focused on its use and utility in sport.

2.1 Canoeing

Canoeing is a nautical sport practised in a kayak or a canoe. These boats were firstly created all around the world by indigenous people that used these crafts to move, to hunt and fish, transport all types of materials, and even for war purposes. The first kayaks probably originate from the artic people, closed boats to ensure that the icy waters of the artic did not enter the boats. On the other hand, canoes were used all over the world, from the first people of North America to Africa and the most remote island natives from New Zealand. These first boats were mostly made of wood, stretched animal skin, and were quite different according to the purpose they were built for [3].

The first competitive races date back to 1869 in Great Britain and were organised by John MacGregor at the British Royal Canoe Club. Later, the first International body for the sport only appeared lately in 1924 in Copenhagen [4].

Nowadays, there are lots of different canoeing boats, however, the most used in competitions are the kayaks and canoes. The main differences between these boats used in canoe sprint are the boat shape, the weight and the type of paddle. Kayaks have an entirely covered deck, and the paddler or paddlers, are seated in an open cockpit and propel themselves with a double-bladed paddle. The kayak also has a rudder to steer the boat. In the case of the canoes, the deck is entirely open, and the athlete or athletes, are paddling bending their knee and propel themselves using a single-bladed paddle. In this boat, the paddler has to steer it using the paddle technique since the boat has no rudder.

The nomenclature used in canoeing is referent to the type of boat used and the number of paddlers in it, so K refers to kayak and C refers to canoe, and the number represents the number of paddlers, for example, ”C2 1000 m ” is referent to a sprint of $1000\ m$ in a canoe with two paddlers in it.

Currently, there are lots of canoeing disciplines such as the marathon, extreme wild water, polo, freestyle, stand up paddle, and many others, but the most relevant ones are the Olympic disciplines Canoe Sprint and Canoe Slalom.

2.1.1 Canoe Slalom

Slalom is an Olympic discipline that consists of a timed event on a whitewater turbulent course with athletes navigating through a combination of up and downstream gates that athletes should not touch, having a time penalty if they do.

The Canoe Slalom event first appeared in the Olympics in 1972 in Munich and it is present in every Olympic event since the 1992 edition in Barcelona [5].

2.1.2 Canoe Sprint

Canoe Sprint is an Olympic discipline in the distances of $200\ m$, $500\ m$, and $1000\ m$. The $5000\ m$ event is also part of the canoe sprint discipline but is not an Olympic event. Sprint events take place in a flatwater course and the athletes are racing against each other in a straight line over the set distance. In canoe sprint, canoes and kayak boats are used and the number of paddlers in it can be 1, 2, or 4.

The Canoe sprint entered the Olympic Games first in the 1936 edition in Berlin and the event is in every event until today. This study will focus on the Olympic event of C1, this discipline has the $1000\ m$ race in men and $200\ m$ in women [4].

2.2 Rules for Canoe Construction

The boat should be perfectly hydrodynamic and ergonomic to the athlete paddle comfortable on it. On the other hand, the boat must respect some rules related to its construction and parameters imposed by the International Canoe Federation (ICF). In this section, the current rules for C1 Sprint construction will be focused on since this project focus on the Olympic discipline of Sprint C1 1000 m.

For the Canoe Sprint, the ICF imposes a maximum length of $5.2\ m$ and a minimum weight of $14\ kg$. It will be enumerated below, in terms of construction parameters, the applicable rules to the C1 boat:

- Steering rudders or any guiding apparatus directing the course of the canoe are not allowed.;
- The C1 may be entirely open. The minimum length of the opening must be $280\ cm$.;
- The edge of the side of the boat (gunwale) can extend a maximum of $5\ cm$ into the boat along with the whole defined opening.;

- The boat can have a maximum of 3 strengthening bars with a width of a maximum of 7 cm each.;
- No canoe section or longitudinal line should be concave, vertically, or horizontally measured.;
- The highest point on the deck must be lower than the highest point of the front edge of the cockpit.;
- Foreign substances that improve canoe performance, are not allowed.;
- Moving parts, including the footrest, that help to propel the canoe are not allowed.;
- Boats should be longitudinal symmetric.;

To guarantee that all boats respect these rules, a boat should be evaluated and accepted first in a boat control in an official World Championship or World Cup, and a new design innovation should be presented to ICF for evaluation until 1 January of the targeted competition year, to be accepted in international competition [6].

2.3 Canoe Design Evolution

Before canoeing entered the Olympic program in Berlin in 1936, the first competition boat designs started to appear, and the first considered era of canoe shapes started at Versuchsanstalt für Wasserbau und Schiffbau (VWS), a research institute for hydraulic engineering and shipbuilding in Berlin. Several boat projects were designed and tested, these first boats were very primordial since there were no regulations at the time.

The first boat regulation arose for the 1948 Olympic Games in London. At this point in time, is when the second era of canoe design started, with boats made of wooden plywood. Back then, boats were ruled by a minimum beam limit rule that limited the design of the canoes. In this era, the competition times started to improve significantly due to the growth of the sport, training, and paddle technique but also due to the improved designs of the boat that emerged.
The third era of canoe design started when no beam limit boats made of composites started to appear, leading ICF to end the beam limit rule in 2003 and open up a whole new range of design opportunities. At this time the competition times started to tend to the current times since the boats started to be much more hydrodynamic and ergonomic [7].

As we can see in Figure 2.1 the times are stabilising, so a hydrodynamic improvement can prove crucial in future winnings. According to Robinson et al. [8], the reduction of the best performance times in kayaking Olympic Sprint events has been reported to be due to improvements in boat design. Of course, these results are always influenced by the weather

conditions. With the current technologies like CFD, engineers can have a better look through boat hydrodynamics and optimise their designs to have less drag and reduce the competition times.

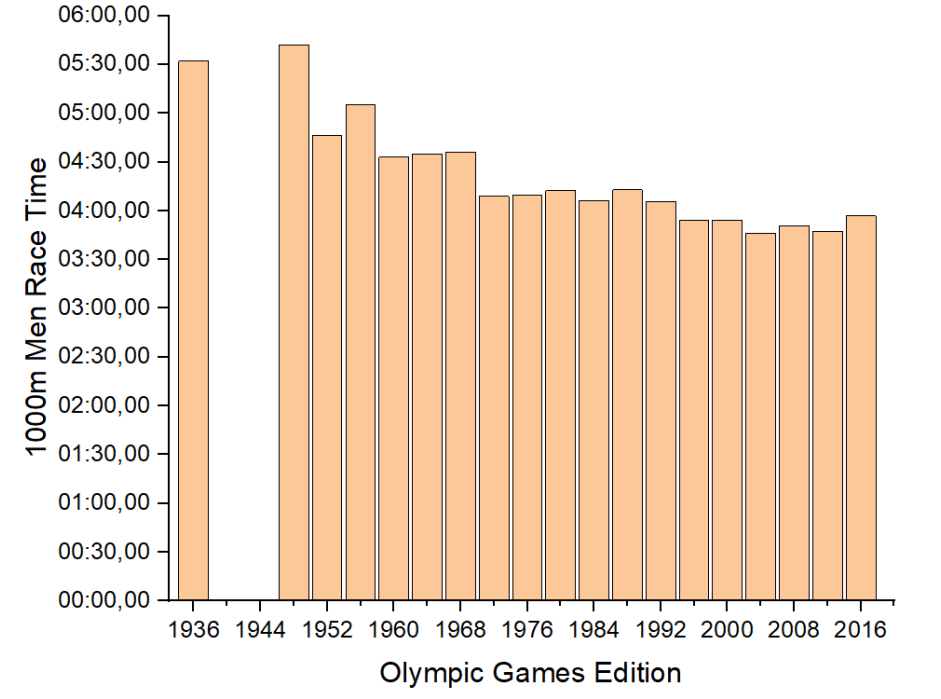

Figure 2.1: Evolution of C1 1000m results throughout the Olympic Games history.

The main design evolution was to narrow the hull shape, that decreased the wet surface area and the frontal area, which in turn have decreased the hull resistance [9]. Nowadays, probably there is no more space to narrow the hull, allowing the athlete to paddle comfortably and stably. Besides, the manufacturers started to develop canoe models with sizes to fit the body weight of the athletes, to be a more personalised boat, allowing the athletes to have a more adapted boat to their characteristics.

In hull design, there are some key factors to consider like hydrodynamic, stability, minimum dimensions, regulations, and paddle ergonomics. These key factors are directly related to design dimensions like length, beam, draught, trim, and block coefficient that will also affect the drag values. These dimensions must be considered when designing the boat because, per example, a much more hydrodynamic boat, but without stability, can have a worse performance.

According to their Froude number, vessels are classified into three types exposed in Figure 2.2 [10]. At lower Froude numbers, there are displacement ships designed to displace as much water as possible, to be stable and efficient moving through water. At higher Froude numbers, vessels are classified as fully planing ships, designed to move faster through water, and at certain velocities designed even to rise on top of water surface to have less drag [11].

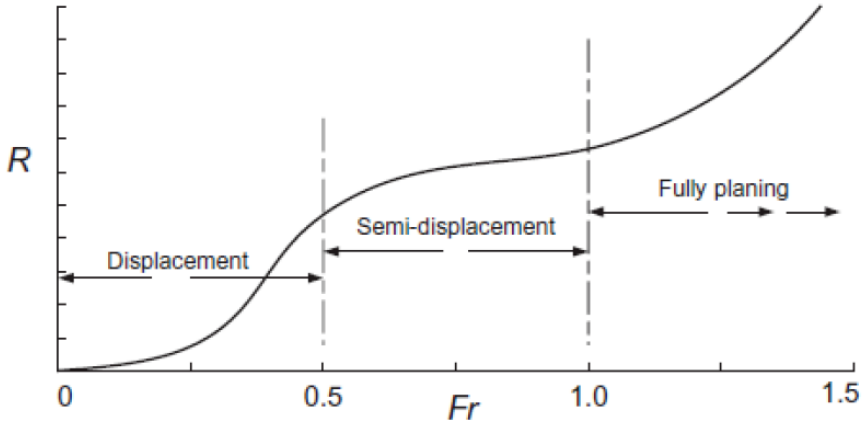

Figure 2.2: Typical Froude Number according to the type of hull. [10].

Typically, due to its Froude number, which is included between 0.471 and 0.728, in ship theory, canoes are considered as semi-displacement ships, which shows that their hydrodynamic parameters are located between high-velocity crafts and planing boats [7]. As a semi-displacement ship, these boats are designed to travel through water at non-planning velocities but generating some lift when moving faster, unlike the displacement ships. Thus, the canoes join velocity characteristics of fully planing boats to the stability of displacement ships at velocities that the athletes can reach [12].

According to this, hull geometries will vary to meet the needs of each boat. There are three classical hull types of geometry exposed in Figure 2.3 [11], and the combination of these geometries, to reach the characteristics that one wants to obtain from each, will lead to new designs.

V-shape hulls are designed to obtain higher velocities, normally sought in planing boats because this geometry allows the boat to quickly accelerate and obtain higher velocities comparing to other hulls. Flat hulls have more stability by having a lower centre of gravity when compared to other hulls. These hulls do not reach higher velocities but, due to their stability characteristics, these are commonly used in canoeing initiation. Round bottom hulls have their bottom round, as the name implies. These hulls travel easily through the water at lower velocities to limit the amount of drag generated by them. These hulls are typically used in displacement ships.

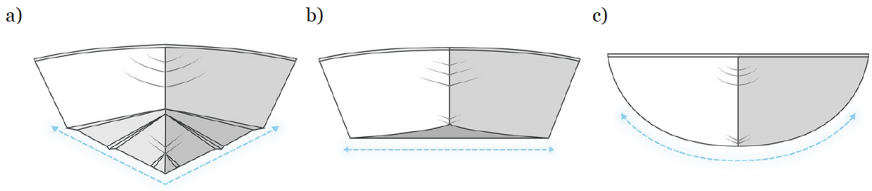

Figure 2.3: Bottom hulls: a) V-shape; b) Flat; c) Round;[11]

Canoe design is obtained by mixing these hulls to obtain the best hydrodynamic lines and stability. It is also important to consider other hull characteristics such as keels (an important characteristic to minimise the course instability), the distribution of volume along the hull's length, and others, to face not only the hydrodynamic but also the efficiency of the athlete paddling.

2.4 Archimedes' principle

This principle, discovered by the ancient Greek mathematician Archimedes, also known as the physical law of buoyancy, will have relevant importance in this case of study since the canoe is a partially submerged body. This principle says that a fully submerged or partially submerged body in a fluid at rest is acted by an upward buoyancy force, with a magnitude equal to the weight of the fluid displaced by the body. This force is the main reason why the canoe floats and it can be represented by the impulse in the following equation:

$$I = \rho g \Delta V \quad (2.1)$$

where I represents the impulse, ρ represents the density of the fluid, in this case, water, g is the gravitational force, and ΔV is the displacement volume of water.

As previously said, the wetted surface area has a determinant role in the drag of the canoe, and it is determined by the depth of the canoe in the water, therefore the waterline level is a crucial factor that will influence the resistance results. The waterline is determined by the bodyweight of the athlete and the buoyancy resulting from the volume distribution and shape of the canoe [13].

2.5 Canoe Hull Drag

In canoeing, one of the most important aspects is the hydrodynamic of the hull. A tenth of a second can be the difference between the gold position or an off podium position, the smallest improvement in the drag of the hull can be the secret of the success of an athlete. An optimum hull will be that which, at a fixed speed, produces the least drag for a given overall weight and length [14].

Drag is defined by the force exerted by the fluid acting in the opposite direction of the body movement. This force will be responsible for the energy consumption to maintain the canoe motion.

In a partially submersed body, drag has two main components, the aerodynamic and hydrodynamic components. This study will focus on the hydrodynamic component since it is the main cause of boat resistance.

Froude hypothesis states that the hydrodynamic component can be divided between friction and residual parts, which are assumed not to interact. Drag is the sum of a frictional drag component, dependent on the Reynolds number, plus the residual drag which is dependent on the Froude number. This makes them two independent components since it is not possible to match both non-dimensional numbers. This impossibility will be shown in Chapter 3. The pressure resistance can be then considered by the sum of the pressure drag and a wave component [14, 15].

Figure 2.4: Hull drag effects on the free-surface, canoe motion back view.

In Figure 2.4, a back view of an athlete paddling, it is possible to analyse the effects on the water of a canoe motion. Along the hull, we can see a wave pattern, as described by Lord Kelvin in 1887 [16], when he performed a study about a wave system generated by the movement of a pressure point at a constant velocity. He found that there was a characteristic pattern where there is a formation of an angle between the centerline of the canoe and the wave crests of approximately 19°degrees, and a line that joins the higher elevation points of the divergent waves that must make an angle of approximately 35°degrees to the same center. These two patterns are visible in Figure 2.4 as an effect of the wave drag.

Also in Figure 2.4, the effects of the friction drag are visible in the wake behind the hull. The region of turbulent flow visible in the wake is built along the hull by the friction between the hull surface and the water [15].

In figure 2.5, the total resistance components of the boat are decomposed. According to

Jackson [14], the main drag components are the frictional resistance, responsible for the highest percentage of the drag, and the wave resistance, another relevant component in the total resistance. In the next subsection, these components will be explained.

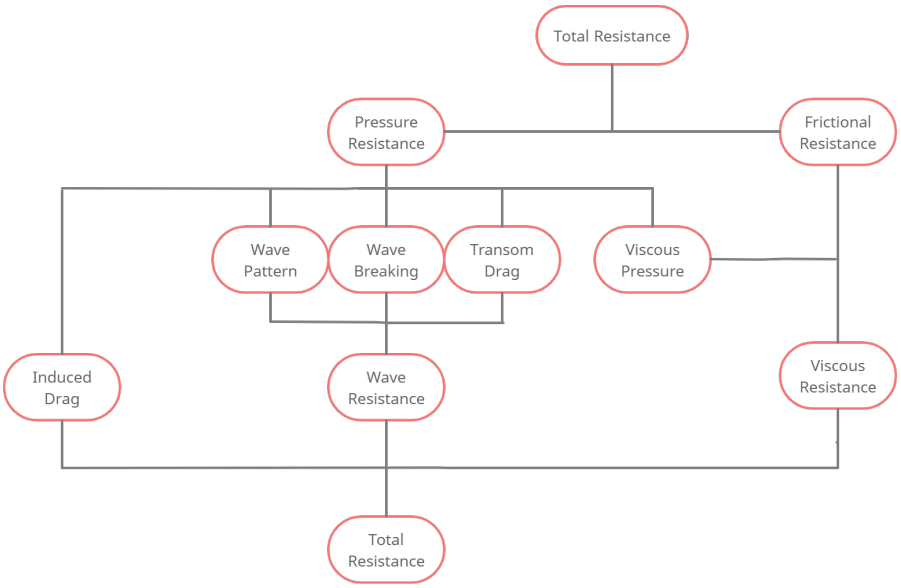

Figure 2.5: Total Resistance Decomposition, adapted from [10]

2.5.1 Frictional Resistance

To predict this resistance force, it was necessary to perform several experimental tests to create functions that reflect the real cases obtained in the experiments.

This component is obtained through the sum of tangential stresses along the wetted surface in the direction of the motion [17]. This component has the most significant participation in the total resistance force at velocities typical from international elite competition, since it is mainly dependent on the wetted area. The draught of the boat is critical in the optimisation of this component. Due to this, according to John Grue at Marine Hydrodynamics foreword, he advised the kayaker Eirik Veras Larsen, to the 2012 London Olympic Games, which he would later win, that the only variable to play within the reduction of drag was the wetted area of the kayak by reducing his body weight [15].
The friction component is given by:

$$D_f = \frac{1}{2}\rho U_H^2 A_{wet} C_f \quad (2.2)$$

where the U_H represents the hull velocity, A_{wet} is the wetted area, and C_f represents the friction coefficient. There are many curves based on experimental data to predict this coefficient, in the bibliography one of the most used is the ITTC-57 formula which is defined by:

$$C_f = \frac{0.075}{(\log \mathrm{Re} - 2)^2} \quad (2.3)$$

where Re represents the Reynolds number. The frictional resistance is directly related to the flow along the hull due to the high Reynolds number in this region. Due to this relation, this coefficient is not only referred to drag resulting from shear forces but to all drag components dependent on the Reynolds number [15]. This non-dimensional number is given by:

$$Re = \frac{U_H L}{v} \quad (2.4)$$

where L is the waterline length and ν is the kinematic viscosity.

Owing to the extreme slenderness of these canoe hulls, the friction drag is probably described more accurately by techniques used for aircraft fuselages than the usual correlation for ship forms [14].

2.5.2 Wave Resistance

The wave resistance component is related to the energy spent in the formation of gravity waves [17]. The study of generated waves by boats moving through water is one of the most important objectives in ship hydrodynamics. At the Froude numbers that the canoes operate, the energy dissipated in the generation of waves is significant. Therefore, this energy dispersion should be reduced by improving the design of the boat [18].

By experimental measurements, it is possible to estimate this resistance through the amplitude of the wave profile. In case there is no experimental data, the residual wave drag depends on the geometric parameters of the hull and the Froude's number. Adler [19] gave a curve for this component as a function of Froude number defined by [14, 19]:

$$D_w = \frac{1}{2}\rho U_H^2 C_w \frac{\Delta^{\frac{5}{3}}}{L^3} \quad (2.5)$$

$$Fr = \frac{U_H}{\sqrt{gL}} \quad (2.6)$$

where C_w represents the residual drag coefficient, and Δ represents the water displacement, which is different for every canoe since it is dependent on the geometrical shape and is reconstructed for some canoes using Adler's curve.

Since the wave-making component of the drag is strictly dependent on his geometrical shape, the design of the hull is a very important step to improve the performance of the boat.

2.6 Total Resistance

The aerodynamic component of the canoe drag is assumed to be mostly due to the crew body since the frontal area of the body is significantly higher than the frontal area of the canoe. It can be defined by:

$$D_a = \frac{1}{2}\rho_a U_H^2 A_a \quad (2.7)$$

where A_a is the sum of athlete and canoe frontal area, and ρ_a is the air density.

In the CFD study, the aerodynamic resistance resulting from the athlete is not considered since it varies on the athlete and does not directly affect the optimisation of the boat performance but only the performance of the athlete. To understand the effect of the hull design on drag, it must be determined without the paddling of the athlete, so the effects of the paddle on the hull flow are not considered either [20].

So, the total drag can be defined as the sum of the previous components:

$$D_T = D_f + Dw + D_a \quad (2.8)$$

2.7 Motion of a canoe

Some aspects that influence the total drag of a canoe are the dynamic changes of displacement and the pitch angle. Before any competition, the mass distribution on a canoe is a very important aspect that should be considered [7]. Beyond the hull drag, these aspects could also affect the stability and comfort of the athlete, which in turn will probably affect his performance.

These motion movements are known by the surge, sway and heave, related to translational movement along to the x, y, and z axes, respectively, whereas the rotational movement in these axes are respectively known as roll, pitch, and yaw, same as for planes [15]. The motions of a canoe are represented in Figure 2.6.

The dynamic changes in the motion of the boat are caused mainly by the paddling but also by many factors, such as free surface waves, wind, imbalances of the athlete, or even mechanical problems related to the boat or paddle. These secondary movements have a particular emphasis by adding additional drag mainly because of the generated gravity wave, which radiates away from the boat dissipating energy [21].

One goal of this study is to understand the effects of the pitch on the canoe hull drag. This motion will raise the front and drop the back of the canoe, or vice versa, causing a pressure differential between its bow and stern, which will affect the pressure drag component. Besides, the wet area may change depending on the pitch, which will influence the frictional

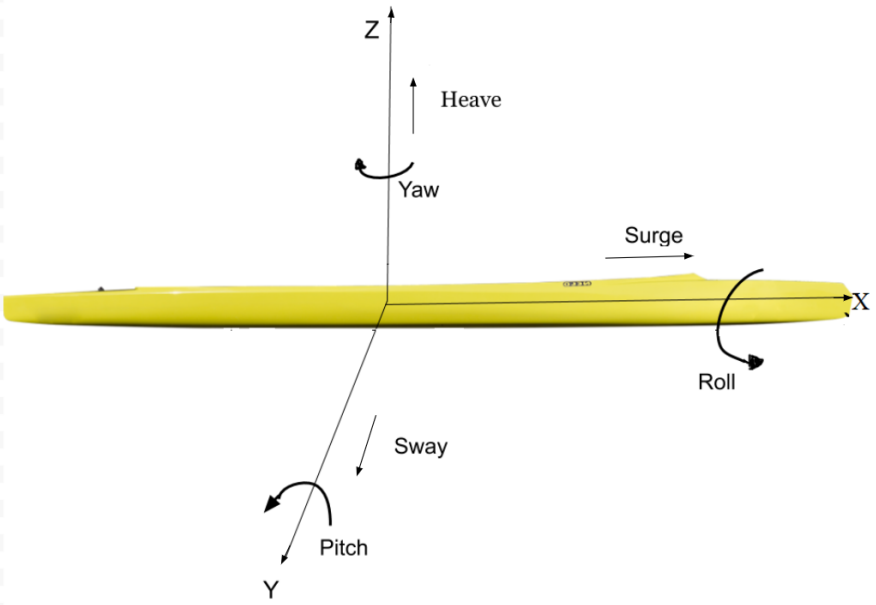

Figure 2.6: Motions of a C1 vessel.

resistance, as previously said in the friction resistance Subsection 2.5.1.

Also, roll and heave could have an important contribution to the final drag resultant. Roll is mainly resulting from the imbalances of the athletes and changes the position of the hull in the water flow, thus having effects on the resulting drag force. The heave will be changing with the paddle movement. During the traction phase of the stroke, the boat tends to sink due to the weight of the body and the force applied to the stroke, increasing the wetted area of the boat. This movement has a significant role in the resultant drag force by increasing both friction and wave drag.

The contribution of these movements, especially heave and pitch, have been neglected in previous studies. In Formaggia et al. [21], the effects of these movements in rowing boats are studied and give a closer approach to the canoe boats.

2.8 CFD in Sport

Computational Fluid Dynamics is a relatively recent computational branch. This tool uses numerical models that were developed at the beginning of the 20th century. Back then, the computational resources were limited, so it was extremely laborious to obtain accurate results of complex cases. With the technology evolution, computational power started to increase, and it started to be possible to solve these numerical models accurately, simulate complex flows and geometries, and have results of interest to predict experimental results.

At the beginning of the decade of 1990, with the first commercial availability of CFD software like FLUENT, some engineers started to use them in sports to improve the equipment design technology and produce a legal competitive advantage improve. Currently, CFD it's a 'must-

have' in sports equipment companies, such as the canoe construction industry [22].

Nowadays, with the evolution of sports engineering, choosing the best equipment, in this particular case, the best boat design, could be as important as choosing the best conditioning program, or even the physical and psychological condition in the athlete performance [20]. CFD simulation is a very important tool in the support of experimental research in hydrodynamics because it is easier to properly compare the influence of flow properties, such as pressure distribution and wave elevation, between different hull designs [7].

In this case study, CFD allows to simulate the flow around the hull and predict the drag values. Also, it is possible to analyse the simulation to see the flow and where the design can be optimised in order to obtain a better performance for the canoe. It is also an advantage, since there is no need to manufacture a model every time you want to test a design change.

The fundamental of CFD and the specifications used in the numerical model will be described at Chapter 4.

Despite the importance of this tool, the performance of experimental tests is relevant, as it allows to validate the numerical simulations. In the next chapter, the methodologies performed in the experimental tests will be described.

Chapter 3

Experimental Study

In this chapter, the procedure to perform the experimental tests, as well as the setup, are explained.

3.1 Introduction

The experimental tests arose from the necessity to get values to validate the obtained numerical results since there are no published data related to the canoe hull resistance.

The experiments were realised at CAR Montemor-o-Velho, an infrastructure that has a class A flatwater course, with an extension of $2000\ m$, width of $135\ m$, and depth of $3.5\ m$, that provided the necessary calm water conditions to perform the tests. The realisation of the tests at this course provided us real condition results, although the environmental conditions, such as wind and surface waves generated by the wind, could affect the results of the experiments. To counteract these factors, it was chosen a day that provide favourable environmental conditions in order to obtain valid results.

The choice to perform the tests on real size, comparatively to test a model, was due to match the Reynolds number and the Froude number and secure similitude between the model and the real size. To get similitude, it is necessary to have geometric similarity, kinematic similarity, and dynamic similarity.

To get dynamic similarity, it is necessary to match both Reynolds and Froude numbers between the model and real size, so we get:

$$Re_R = Re_M \Leftrightarrow \frac{\rho U_R L_R}{\mu} = \frac{\rho U_M L_M}{\mu} \Leftrightarrow U_M = \frac{U_R L_R}{L_M} \quad (3.1)$$

$$F_{r_R} = F_{rM} \Leftrightarrow \frac{U_R}{\sqrt{g L_R}} = \frac{U_M}{\sqrt{g L_M}} \Leftrightarrow U_M = U_R \sqrt{\frac{L_M}{L_R}} \quad (3.2)$$

where Re_R and Re_M is the Reynolds number of the real size and model, respectively, F_{r_R} and F_{rM} are the Froude number of the real size and model, respectively, U_R and $U_M$are the velocity of the real and model, respectively, L_R and L_M are the length of the real size and the model, respectively. Since the fluid is water for both real size and model, density and dynamic viscosity are equal.

Therefore, to have dynamic similarity, both model velocities obtained from the Reynolds and Froude number have to match.

$$U_M = U_M \Leftrightarrow \frac{U_R L_R}{L_M} = U_R \sqrt{\frac{L_M}{L_R}} \quad (3.3)$$

$$\frac{L_R}{L_M} = \sqrt{\frac{L_M}{L_R}} \Leftrightarrow \frac{L_R^2}{L_M^2} = \frac{L_M}{L_R} \Leftrightarrow L_R^3 = L_M^3 \Leftrightarrow L_R = L_M \quad (3.4)$$

To get dynamic similarity, the length ratio should be 1, therefore, the experimental tests must be done in real size. Due to our ease of access to these vessels and the difficulty of finding an available towing tank that satisfied the dimensions of the domain necessary for the analysis, it was decided to do the tests in real size.

In the literature, there are very few experimental tests realised related to the drag of hull and most of them are realised for the hull of the kayak. In Bugalski [7], tests were performed to analyse the hull of the canoe, at a towing tank in real size, but the results are not disclosed. Other studies such as Bible [23] and Tzabiras et al. [24] performed real size experimental tests to determine the drag of the hull. In Bible [23], a cable-car mechanism was attached to the K1. In Tzabiras et al. [24], a running carriage was attached to the K1, both tests were performed in a towing tank with only one boat model tested and one single paddler body weight. At Gomes et al. [20, 25], experimental tests are performed to obtain drag data related to K1, testing different models and different body weights at Montemor-o-Velho.

3.2 Experimental Facility

The field towing system is described accurately at Gomes et al. [20], as it is composed of a sliding platform with an electromechanical device attached. This device is composed of a $559\ mm$ drum driven by a $750\ W$ electric motor (Direct Drive) that will pull the canoe. The drum has a variable power source controlled by a hand accelerator, allowing to change the angular velocity of the drum. To measure the resistance force, the drum was also attached to a load cell (iLoad, Loadstar) by a steel cable, which in turn is attached to a fixed point behind the device at the same height as the centre of the drum, as showed in Figure 3.1. [20, 25]

The kayak velocity was measured by a calibrated wireless speed meter (BC 8.12, Sigma Sport) positioned on the wheel to determine its revolution rate. This speed meter was calibrated by measuring the ”roll-out”, as suggested by the manufacturer. To pull the canoe, an inelastic cable that was $300\ m$ in length (Caperlan), $0.8\ mm$ diameter, $180\ g$ total weight and made of fluorocarbon, was used and attached to the canoe. The load cell data was linked to the PC, to receive and process the data obtained from the experiment. The force data were sampled at $50\ Hz$ using LoadVue software (Loadstar). The accuracy of the load cell, according to the manufacturer, is $\pm 0.2\%$.

Figure 3.1: Field-towing system used in the experimental tests.

3.3 Data Collection

The model used in all tests was Nelo C1 5 L and Nelo C1 8 L, both used in sprint and marathon races. According to the manufacturer, the recommended weight range for these canoes size is between $70 - 80\ kg$. Both canoes have the same length ($5.2\ m$), overall weight ($14\ kg$), and have the same construction materials and methods. The position of the athlete in the boat was set to maintain a neutral position, with a pitch angle of 0 degrees.
During the data collection, there was no significant wind or surface waves that could affect the final results.

The athlete was asked to maintain a vertical and static body position and do not touch the water with the paddle. The athlete held a paddle to help him remain balanced, which was a difficult task due to the natural instability of these competitive boats in a static position.

Another difficulty was to maintain the trajectory of the boat. This was solved by placing a guide on the bow of the boat so that the string does not deviate from the intended path. Also, due to the force exerted on the wire and to the usage, after successive tests, sometimes the wire broke. After each test, or whenever the wire broke, it would have to be replaced in the system. This repetitive process, after several tests become tiring, could be something to be taken into account to improve the system.

3.4 Methodology

The participants chosen were elite athletes of $80\ kg$ and $90\ kg$, both to be towed in a linear competitive flatwater course. The ideal situation would be to do the experimental tests using the same $80\ kg$ athlete, however, the athlete was not available to do the tests on the second boat.
The canoes utilized in the experimental tests are the Nelo C1 8 L (Figure 3.2) and the Nelo C1 5 L (Figure 3.3), the same models and sizes as the geometries provided by Nelo (M.A.R. Kayaks Lda., Portugal) for this study.

Figure 3.2: Nelo C1 8 L, Side view.

Figure 3.3: Nelo C1 5 L, Side view.

The experimental setup from Gomes et al. [20] and Oh et al. [26] was only adapted from the kayak boat to the canoe boat. It was utilised the same specially designed field-towing system in Gomes et al. [20] located on land, assembled as in Figure 3.4.

The athlete remains still in the canoe, not paddling, only to stabilise it in order to collect the hull drag data only. The data collection made over $250\ m$ distance, to have a required time period to stabilise the velocity, and collect the data only when the boat is in a linear trajectory with fully stretched wire, to guarantee to have accurate results of the hull drag.

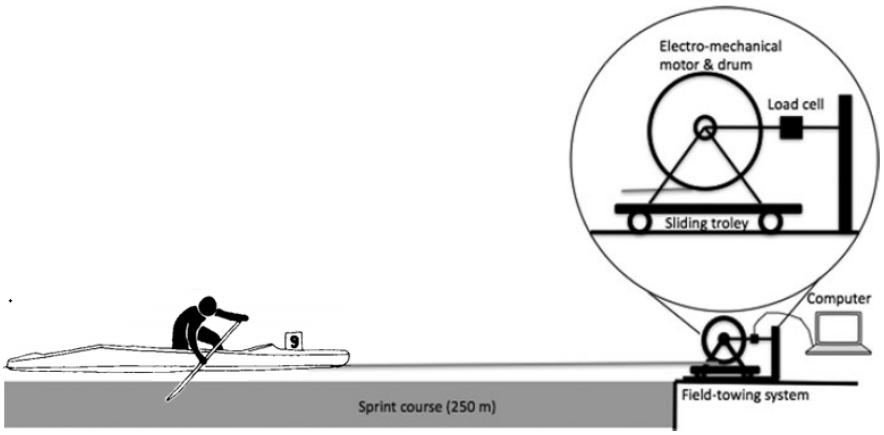

Figure 3.4: Experimental Setup adapted from Gomes et al. [20].

Chapter 4

Mathematical Model

In this chapter, it will be reviewed some important fluid mechanics fundaments, as well as the governing equations and methods used later in the numerical model.

4.1 Governing Equations

As previously said, fluid flow can be described by basic classical physical principles and conservation equations, governing equations, these must be reviewed before the formulation of the numerical problem. The governing equations of fluid flow are given by the following conservation laws:

- Mass.
- Momentum conservation or Newton's Second Law.
- Energy.

These equations are fully described in all forms [27, 28].

To simulate the motion of the canoe with steady velocity is used an Eulerian method by keeping the canoe static while the fluid flow at a constant velocity, generating a turbulent flow around the canoe hull due to a high Reynolds number between the order of 5 and 6 [29]. As a Newtonian incompressible fluid flow, this study can be fully described by the Navier-Stokes and continuity equations in the simplified forms given by:
Continuity equation:

$$\frac{\partial u}{\partial x} + \frac{\partial v}{\partial y} + \frac{\partial w}{\partial z} = 0 \quad (4.1)$$

where u, v and z represents the three component of the velocity.
Navier-Stokes equations:

$$\begin{aligned}
\rho\left(\frac{\partial u}{\partial t} + u\frac{\partial u}{\partial x} + v\frac{\partial u}{\partial y} + w\frac{\partial u}{\partial z}\right) &= -\frac{\partial p}{\partial x} + \rho g_x + \mu\left(\frac{\partial^2 u}{\partial x^2} + \frac{\partial^2 u}{\partial y^2} + \frac{\partial^2 u}{\partial z^2}\right) \\
\rho\left(\frac{\partial v}{\partial t} + u\frac{\partial v}{\partial x} + v\frac{\partial v}{\partial y} + w\frac{\partial v}{\partial z}\right) &= -\frac{\partial p}{\partial y} + \rho g_y + \mu\left(\frac{\partial^2 v}{\partial x^2} + \frac{\partial^2 v}{\partial y^2} + \frac{\partial^2 v}{\partial z^2}\right) \qquad (4.2) \\
\rho\left(\frac{\partial w}{\partial t} + u\frac{\partial w}{\partial x} + v\frac{\partial w}{\partial y} + w\frac{\partial w}{\partial z}\right) &= -\frac{\partial p}{\partial z} + \rho g_z + \mu\left(\frac{\partial^2 w}{\partial x^2} + \frac{\partial^2 w}{\partial y^2} + \frac{\partial^2 w}{\partial z^2}\right)
\end{aligned}$$

4.2 Multiphase Flow Modeling

Since the canoe is moving through two fluids in two different phases, air and water, the VoF (Volume of Fluid) method is implemented to solve the free surface interface between both fluids.

In this methodology, in each control volume, the volume fractions of all phases sum to unity, so the fields represent volume-averaged values for the phases. A cell is full of a certain fluid, if its volume fraction is equal to 1, in this case, 1 represents it is full of water. If the volume fraction is equal to 0, that cell is empty of that fluid, in our case is full of air. When the volume of fraction is between 0 and 1, it represents that the cell is at the interface between that fluid and another fluid.

This numerical method can model the interface between both fluids and solve the momentum equations and track the volume of fraction of each fluid through the domain. For a q^{th} phase, the momentum equation has the following form:

$$\frac{1}{\rho_q}\left[\frac{\partial}{\partial t}\left(a_q\rho_q\right)+\nabla\cdot\left(a_q\rho_q\overrightarrow{v_q}\right)=S_{a_q}+\sum_{p=1}^{n}\left(\dot{m}_{pq}-\dot{m}_{qp}\right)\right] \quad (4.3)$$

where $\dot{m}_{qp}$ is the mass transfer from phase q to phase p and $\dot{m}_{pq}$ is the mass transfer from phase p to phase q. In this case, there is no mass transfer, so the equation is simplified, a single momentum equation is solved throughout the domain, and the velocity field is shared among the phases. For the momentum equation we get:

$$\frac{\partial}{\partial t}(\rho\vec{v})+\nabla\cdot(\rho\vec{v}\vec{v})=-\nabla p+\nabla\cdot\left[\mu\left(\nabla\vec{v}+\nabla\vec{v}^{T}\right)\right]+\rho\vec{g}+\vec{F} \quad (4.4)$$

The mass conservation equation is given by:

$$\nabla\cdot\vec{U}=0 \quad (4.5)$$

In a two-phase system, as our case study, the density and viscosity in each cell are given by:

$$\rho=\alpha_2\rho_2+\left(1-\alpha_2\right)\rho_1 \quad (4.6)$$

$$\mu=\alpha_2\mu_2+\left(1-\alpha_2\right)\mu_1 \quad (4.7)$$

where ρ represents the density, μ represents the viscosity, and α represents the volume of fraction, being that 1 and 2 represent each phase, water and air, respectively.

To simulate this case study, it was used the Open Channel Flow model that uses VOF formulation and the open channel boundary condition, like a river or a canoe flatwater course. This flow is characterised by the Froude number, which was previous explained in 2.5.2. Based on this non-dimensional number, this case study is classified as subcritical. Since Fr<1, and disturbances can travel upstream as well as downstream, and downstream conditions might affect upstream conditions.

4.3 RANS Equations

The turbulent flows are hard to describe, due to all the chaotic events happening in the flow. Directly simulating these flows is extremely computationally expensive, so the resolution of the small scale frequency fluctuations is removed to obtain less computational equations to solve. These simplifications are known as turbulence modelling.

There are four main types of ways to solve these turbulent flow, the Reynolds-averaged Navier-Stokes equations (RANS) models, Detached Eddy Simulation (DES), Large Eddy Simulation (LES), and Direct Numerical Simulation (DNS), ordered from the less to more computationally expensive, but also from less to more accurate.

In this dissertation, RANS equations were used to simulate this case, since they are less computationally expensive, based in statistical averaging, and can provide the necessary information to obtain conclusions from this case of study.

In the RANS model, the turbulent effects are replaced by time-averaged estimatives, so the velocity components are represented by the sum of its mean velocity plus the fluctuating velocity. Therefore, the velocity components are presented in the following equation:

$$u_i = \bar{u}_i + u_i' \quad (4.8)$$

where $\bar{u}_i$ represents the mean velocity and u_i' the fluctuation of the velocity component $(i = 1, 2, 3)$.

For the other scalar quantities such as pressure, energy, or species concentration the representation will be the same:

$$\phi = \bar{\phi} + \phi' \quad (4.9)$$

where ϕ represents a scalar quantity.

So, if we substitute the expression of this form, for the flow variable into the instantaneous continuity and momentum equations, we will get the Reynolds-averaged Navier-Stokes (RANS)

equations:

$$\frac{\partial \rho}{\partial t} + \frac{\partial}{\partial xi}\left(\rho u_i\right) = 0 \quad (4.10)$$

$$\frac{\partial}{\partial t}\left(\rho u_i\right) + \frac{\partial}{\partial x_j}\left(\rho u_i u_j\right) = -\frac{\partial p}{\partial x_i} + \frac{\partial}{\partial x_j}\left[\mu\left(\frac{\partial u_i}{\partial x_j} + \frac{\partial u_j}{\partial x_i} - \frac{2}{3}\delta_{ij}\frac{\partial u_l}{\partial x_l}\right)\right] + \frac{\partial}{\partial x_j}\left(-\rho\overline{u_i' u_j'}\right) \quad (4.11)$$

The velocities and other variables now represent the time-averaged values in these equations, the additional terms now appear that represent the turbulence effects [27].

4.4 K-epsilon Turbulence Model

In terms of turbulence models, *"no single turbulence model is universally accepted as being superior for all classes of problems"*, therefore, the choice of model is based on available resources, time, and necessity of the study.

This is the most used turbulence model in engineering industrial applications because of its robustness and satisfactory accurate results for turbulent flows relative to his computational economy. Therefore, for this dissertation, the Standard $\kappa - \varepsilon$ model was chosen, being that it can provide the necessary precision for the study, while it is not computationally expensive when compared to other turbulence models. This model calculates the turbulent length and time scale by solving two equations, the turbulent kinetic energy equation (κ) and dissipation rate equation (ε). These values are obtained from the following transport equations:

$$\frac{\partial}{\partial t}(\rho k) + \frac{\partial}{\partial x_i}\left(\rho k u_i\right) = \frac{\partial}{\partial_{x_j}}\left[\left(\mu + \frac{\mu_t}{\sigma_k}\right)\frac{\partial k}{\partial x_j}\right] + G_k + G_b - \rho\varepsilon - Y_M + S_k \quad (4.12)$$

and

$$\frac{\partial}{\partial t}(\rho\varepsilon) + \frac{\partial}{\partial x_i}\left(\rho \in u_i\right) = \frac{\partial}{\partial x_j}\left[\left(\mu + \frac{\mu_t}{\sigma_\varepsilon}\right)\frac{\partial \varepsilon}{\partial x_j}\right] + C_{1\varepsilon}\frac{\varepsilon}{k}\left(G_k + C_{3\varepsilon}G_b\right) - C_{2\varepsilon}p\frac{\varepsilon^2}{k} + S_e \quad (4.13)$$

where G_k represents the generation of turbulence kinetic energy due to the mean velocity gradients, G_b is the generation of turbulence kinetic energy due to buoyancy, Y_M is the contribution of the fluctuating dilatation in compressible turbulence to the overall dissipation rate, $C_{1\varepsilon}$, $C_{2\varepsilon}$, $C_3\varepsilon$ are constants, σ_k and σ_ε are the turbulent Prandtl numbers for k and ε, respectively. S_k and S_e are user-defined source term. The turbulent viscosity, μ_t is obtained through k and ε by:

$$\mu_t = \rho C_\mu \frac{k^2}{\varepsilon} \quad (4.14)$$

where C_μ is a constant.

Since we are using the standard model, the constants $C_{1\varepsilon}$, $C_{2\varepsilon}$, C_μ, σ_k and σ_ε have the following default values [27, 30]:

Table 4.1: Turbulence models constants.

$C_{1\varepsilon}$	1.44
$C_{2\varepsilon}$	1.92
C_{μ}	0.09
σ_k	1.0
σ_{ε}	1.3

In the following sections, it will be described the numerical procedure applied in the simulations, such as the workflow, pre-processing tasks, boundary conditions, and the mesh independence test.

4.5 Numerical Model

As previously said, CFD is used to predict the fluid flow by solving numerically a set of governing equations that were previously exposed. To solve these equations, Ansys Fluent software is used. Also, Ansys Workbench, where Ansys Fluent belongs, offers software utilities to create the fluid domain, create the mesh, and post-processing.

Ansys Fluent is an industry-leading fluid simulation software in the sports field, particularly in the sports equipment and water sports boats, engineers have been using Ansys numerical simulation of the software to optimise the fluids dynamics for these boats, and this software showed up to be a crucial part of the designs process of these equipment's and simulate the flow around it [30, 31].

To simulate this case study, this software solves these equations based on the finite volume method. Based on this, the domain must be discretised into a finite set of control volumes and, the governing equations are solved for this set of control volumes. The general transport equation is defined by the following equation:

$$\frac{\partial}{\partial t}\int_V \rho\phi dV + \oint_A \rho\phi V \cdot dA = \oint_A \Gamma_\phi \nabla_\phi \cdot dA + \int_v S_\phi dv \quad (4.15)$$

The first term of this equation represents the unsteady component, the second is the convection component, the third one represents the diffusion and finally, the last term is the generation of energy. Then, the partial differential equations are discretised to a system of algebraic equations and numerically solved to render the solution field.

The workflow of a CFD typically follows the model as in Figure 4.1:

The first step should be the problem identification. A physical problem must be transformed into a mathematical formulation that represents the real problem. In order to save computational cost and transform the physical problem into a mathematical problem possible to solve, some assumptions and simplifications must be done but taking into account that these

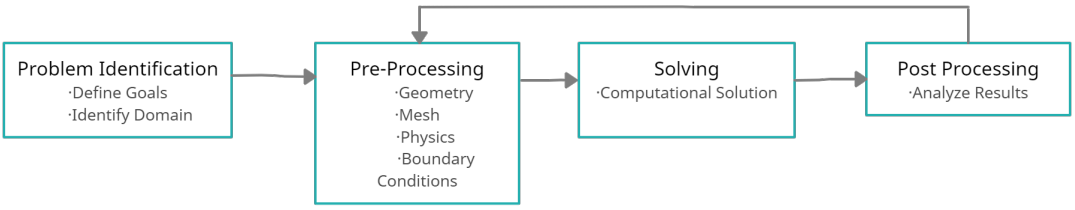

Figure 4.1: Adopted CFD Workflow.

doesn't affect the final result.

In the pre-processing step, the flow should be described to the CFD program by creating a computational domain. Since it is a finite volume method problem, it should be described how the control volume is arranged, the meshing. Also, the physics of the fluid and properties should be described such as the solver settings and the boundary condition of the problem.

The next phase is when the software solves numerically the mathematical problem, outputting the computational solution.

The last phase of the workflow is post-processing, where the flow and its properties are analysed. In the case of this work, the resistance of the canoe is the main goal. In this phase, the problem solution is presented. This solution should show a more intuitive answer for the flow.

So, as previously mentioned, some steps and choices must be made in order to validate the numerical procedure and obtain reliable results. In the next section, all these steps will be explained.

4.6 Pre-Processing

Following the CFD workflow previously showed in image 4.1, firstly, both geometries were prepared. The initial geometries were provided by NELO M.A.R. Kayaks, acquired through a standard commercial L.A.S.E.R. scanner. These geometries had to be worked on since some simplifications must be done to analyse the flows around them, without diverging the result. Due to that, it was necessary to correct some imperfections in the geometry and smooth some lines, which are result from acquiring the geometries from 3D scanner.

Firstly, the initial geometries were prepared on Catia V5, where only the hull part was preserved. Since we are focused on the hydrodynamics as the main drag component, only the hull will be analysed to simplify the geometry. Also, to save computational cost, the canoe was split in half due to its longitudinal symmetry, and only half of the hull will be analysed. This symmetry assumption is reasonable since we are studying a steady-state flow and greatly simplifies the calculations. This presents an advantage on computational cost since the sim-

ulation becomes around four times lower [32]. Also, paddling is not considered since the paddle movement through water could result in a yaw movement that could become relevant in the case of sweep the boat.

The canoe was filled with the material inside in order to simplify the calculation since the airflow inside the canoe is neglected. This airflow calculation in some corners and very small areas could diverge the solution, and its simplification does not alter the final result. Also, it would entail a higher computational cost. In Figure 4.2 is showed the transformation made on Catia V5 from the initial provided geometry to the final one for the C1 5 L case. The same was done to C1 8 L.

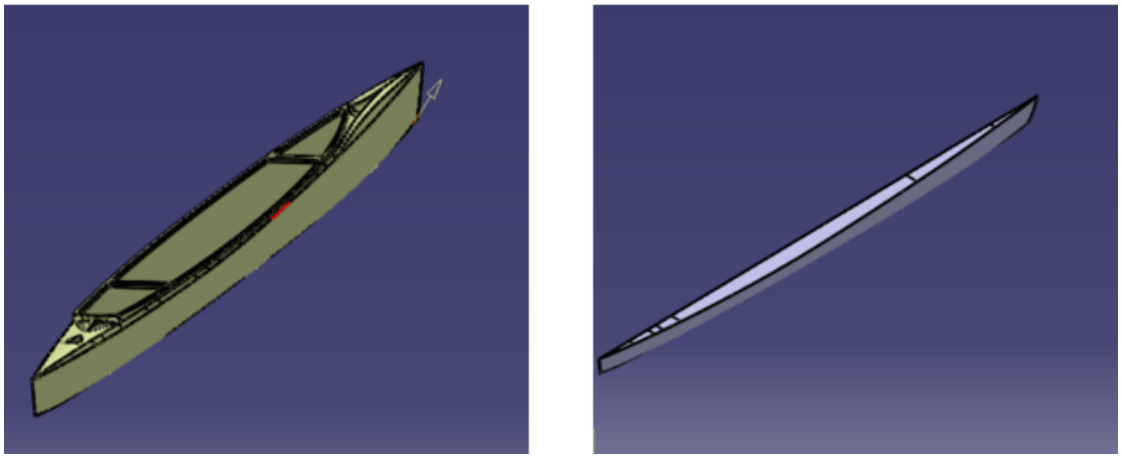

Figure 4.2: Isometric view of C1 5 L initial and final geometries at Catia V5.

4.7 Computational Domain

After the geometry was prepared, the flow domain was created. The domain has to guarantee that the flow has full development without being compromised by the walls of the domain.

As previously said, due to the longitudinal symmetry in the geometric shape of the canoe, the domain will only consider half of the canoe domain.

The upstream boundary is located at $5.2\ m$ of the boat bow, one canoe length. This distance may be sufficient since the flow is mostly unperturbed before it touches the bow of the canoe. The downstream distance must be bigger since the flow in the back of the stern is more disturbed by the passage through the hull, so the distance of the back boundary will be bigger than twice the size of the canoe length. The lateral boundary of the domain was fixed approximately about one length of the canoe due to the same reason as the back boundary, to fully develop the flow without the lateral wall interference. The down boundary was set at $3\ m$, the minimum depth used typically used in the tracks. The upper boundary was set at $1\ m$ due to the low interference of the aerodynamic component in the final result of drag estimation and to save computationally cost.

The boundary conditions applied in this study will be shown in Figure 4.3, matching with the explanations given for the dimension of the domain.

The simulation of the canoe moving with steady velocity is implemented by keeping the canoe static in the fluid flowing at a constant velocity from the domain inlet. To the simulation of the pitch angle, the canoe is rotated through its centroid.
The domain was set to predict a free surface, but the study of the drag was simplified by not

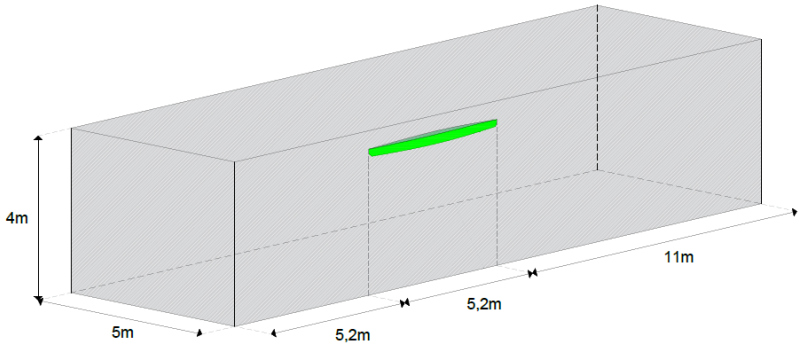

Figure 4.3: Created Domain dimensions.

considering the effects of the paddle in hull flow, surface wind waves, generally present in real conditions. The contribution of these simplifications is assumed to be less predominant and is assumed to be within 10% of the total drag, similar to the drag contributed by air on the athlete and upper portion of the canoe, in the case of the surface wind waves [14, 29], and the case of the effects of the paddle, is also assumed to be less predominant than the aerodynamic effects. These effects would also depend on the athlete technique, cadence and used blade [14, 33].

4.8 Boundary Conditions and Flow Modeling

In Figure 4.4, are shown the boundary conditions of the domain. A pressure inlet and pressure outlet were implemented in the Upstream and Downstream, respectively. The walls on the lateral, superior, and inferior boundaries are considered as far-field flow to avoid the influence of its viscous effects on the remaining flow. The lateral wall location was calculated to conclude that the distance from the walls to the hull would not influence the results, based on the surface wave angle created by the hull explained in Section 2.5.2. The hull zone is considered a no-slip stationary wall to model the effects of the flow in the hull and their drag effects.

The flow velocity was set based on typical race velocity to be in a podium position, according to the previous World Championships male $1000\ m$ results, to perform the mesh independence test. After that, the velocity is varied from $3.33\ m/s$ to $5.56\ m/s$.

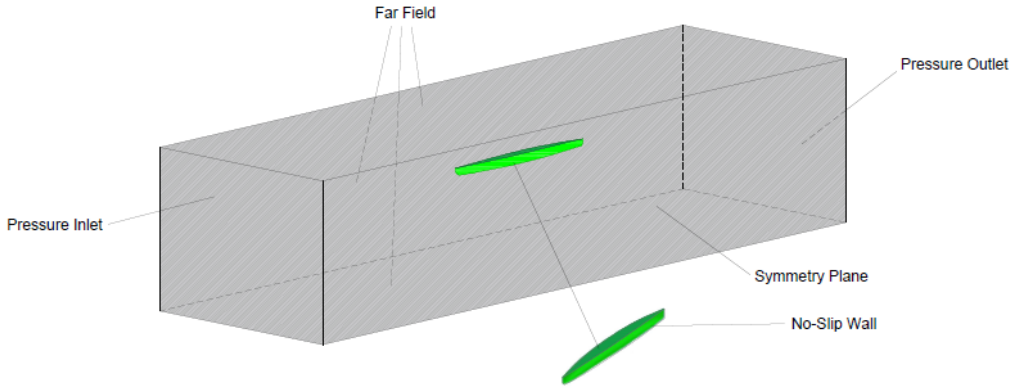

Figure 4.4: Domain Boundary Conditions

.

Table 4.2: Fluid properties at 20ºC.

Fluid	**Density** $[\mathrm{kg/m^3}]$	**Viscosity** $[Pa \cdot s]$	**Surface tension** $[mN/m]$
Air	1.225	1.825e-05	-
Water	998.8	0.001	72.86

Since we are modelling a multiphase flow, two phases were used, air and water, with a constant surface tension between them, fixed on 72.86 $mN \cdot m^{-1}$. The properties of these two fluids are those established at 20ºC.

Based on the literature and tests that have been done, it was decided to use the two-equation Standard $\kappa - \varepsilon$ turbulence model in these steady simulations, given its good capability to predict the viscous effects on the boundary layer. This model, in comparison to the $\kappa - \omega$ model, uses less computational resources, needing more refinement in the hull zone to respect the established parameters for $y+$.

The turbulence intensity was set to 0.05%, the standard values for free stream flows. For the turbulence length scale, it was set to be 7% of the body length, in this case, at $0.364\ m$, which is used for approximation for a flow across an obstacle [27]. The convergence criteria adopted for this numerical simulation was 10^{-3} in residuals.

To solve the problem, the coupled scheme algorithm is used. This scheme will solve the flow in a coupled manner, solving the momentum and pressure based continuity equations simultaneously.

For the gradient discretisation, the Least Squares cell-based method is used. In the pressure discretisation case, PRESTO! is used. First-order upwind is utilised in the momentum,

turbulent kinetic energy, and turbulent dissipation rate discretisation. For the VoF reconstruction scheme, the Compressive method was used.

4.9 Mesh

After defining the fluid domain, it must be divided into smaller elements so that the software solves the governing equations for each element via the method of finite volumes. To do this decomposition into smaller elements, Ansys Meshing was used to create the mesh on the domain.

Some parameters should be considered when doing the meshing process, such as the domain size, mesh size, and distance of the first layer of the cells to the hull. This last parameter, the distance of the first layer cells, is also known as the y^+ parameter, a dimensionless number from the surface of the body to the near-wall node, given by:

$$y^+ = \frac{y \cdot \mu^*}{v} \quad (4.16)$$

where y represents the distance of the first layer cells to the hull, μ^* is the friction velocity, and ν represents the local kinematic viscosity of the fluid.

This friction velocity can be given by:

$$\mu^* = \sqrt{\frac{\tau_w}{\rho}} \quad (4.17)$$

where τ_w represents the shear stress and ρ the density.

Since we are using the Standard $\kappa - \varepsilon$ model, the calculation of the boundary layer is substituted by a wall function to reduce the computational cost, so the acceptable values for the range of y^+ in this model, to accurately simulate the flow near the wall and give a reliable prediction of the turbulent flow, is between 30 and 300 [27].

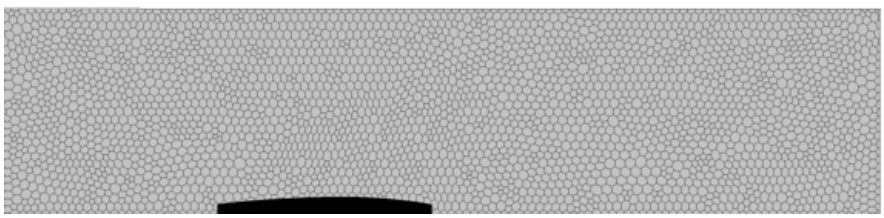

Figure 4.5: Top mesh view.

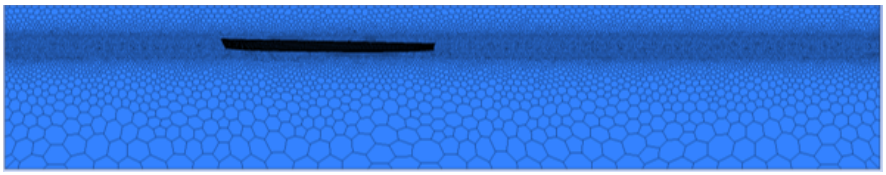

Figure 4.6: Side mesh view.

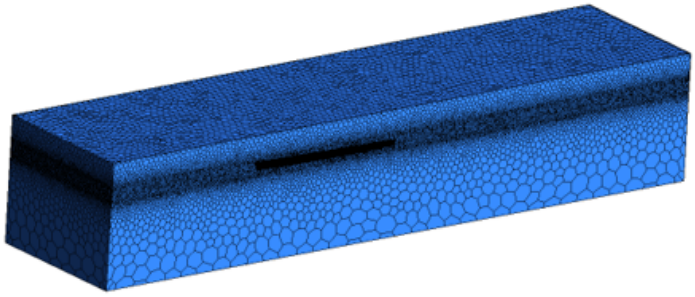

Figure 4.7: Isometric Mesh view.

The mesh was designed to have three main zones represented by three layers as seen in Figure 4.7. An unstructured mesh is used in the top and bottom layer without much refinement since these zones do not need it due to the distance to the hull. An unstructured mesh in the water-air interface layer is also used, more refined, to better represent the free surface and the hull wake effects as seen in Figure 4.6 [34].

In the hull zone, a structured grid even more refined is adopted. A bias factor is used to respect the $y+$ parameters. This zone is visible in Figure 4.8.

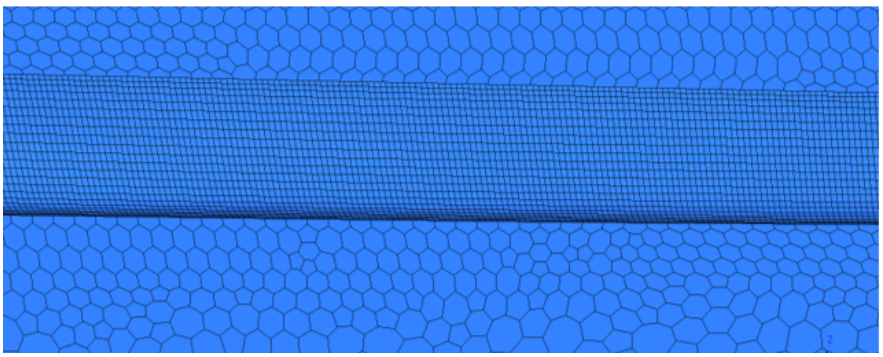

Figure 4.8: Hull zone mesh enhanced.

Also, the mesh domain was converted from Tetrahedral to Polyhedral mesh to reduce the computational cost.

When the setup and boundary conditions are done, it must be guaranteed that the resulting

mesh assures us the veracity of the intended results. Due to this, the independence of the results from the mesh must be verified, which occur when the results with a refined mesh are similar to the previous ones from less refined meshes.

During the advance of mesh refinement, the size of the elements were all downsized by the same ratio. The first layer elements around the body remain the same to assure that the $y+$ parameters, previously explained, are accomplished. Following this, the body elements will be grown from the body until the free stream region according to the mesh design.

Although the same methods have been used in both geometries, the mesh independence study is performed for both because due to their different geometries, the mesh obtained is not equal. The mesh independence study was performed for both canoes' geometries at $4.44\ m/s$ and zero degrees pitch by calculating its resistance. Figure 4.9 shows the mesh independence study on resistance for C1 5 L. In this graphic, it is visible that drag results converge after 12 Million elements, since there is no considerable variation on the drag results, so considering the computational cost, it is used a 12 million elements case in future simulations.

In the case of Figure 4.10, it is visible that the drag results start to converge after 14 million elements, since there is no significative variation after that. So, in the C1 8 L case, it is used the 14 million elements case in the simulations.

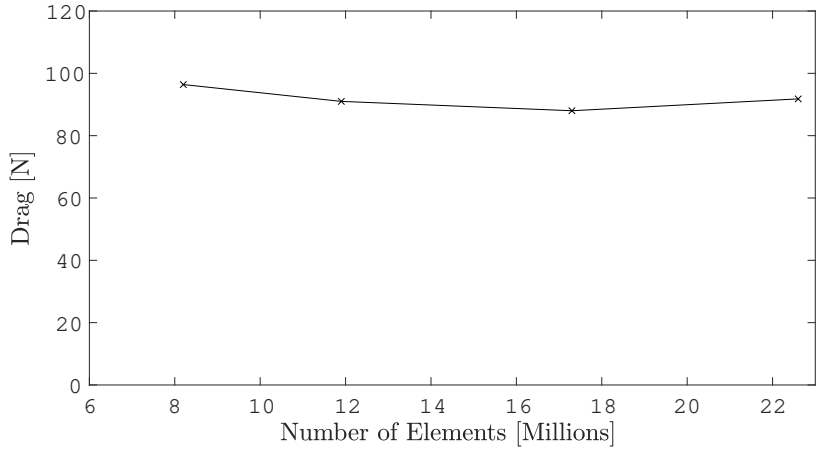

Figure 4.9: Mesh Independence Study of the C1 5 L for drag values.

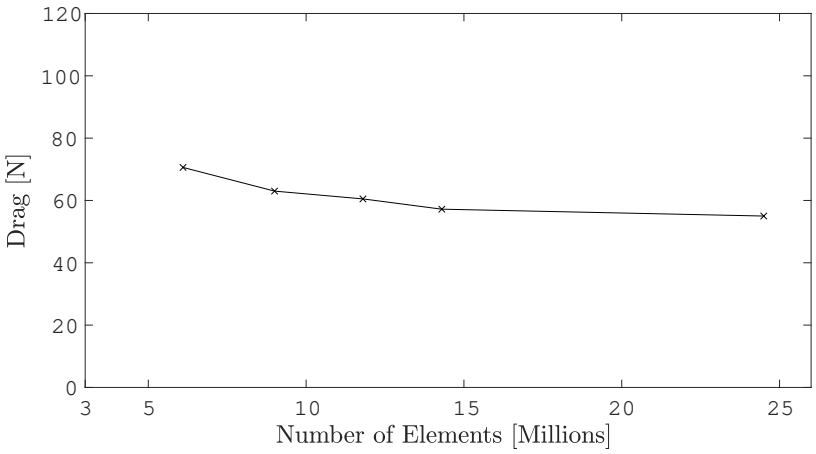

Figure 4.10: Mesh Independence Study of C1 8 L for drag values.

Chapter 5

Results and Discussion

In this chapter, it will be presented the obtained results for the numerical simulations. In the first sections, both models are analysed separately, and compared to their experimental results to validate the simulation results.

The following section directly compares and analyses the flow contours for velocity and wave elevation to understand the differences between both hulls effects, in the free-surface. Finally, it is analysed the effects of the pitch angle in the drag of the hull.

5.1 Comparison with Experimental Results

5.1.1 C1 5 L model

The drag variation with velocity results for C1 5 L model is shown in Figure 5.1. There are two waterlines shown, one located $90\ mm$ below the top of the boat and another located $100\ mm$ below the top of the boat.

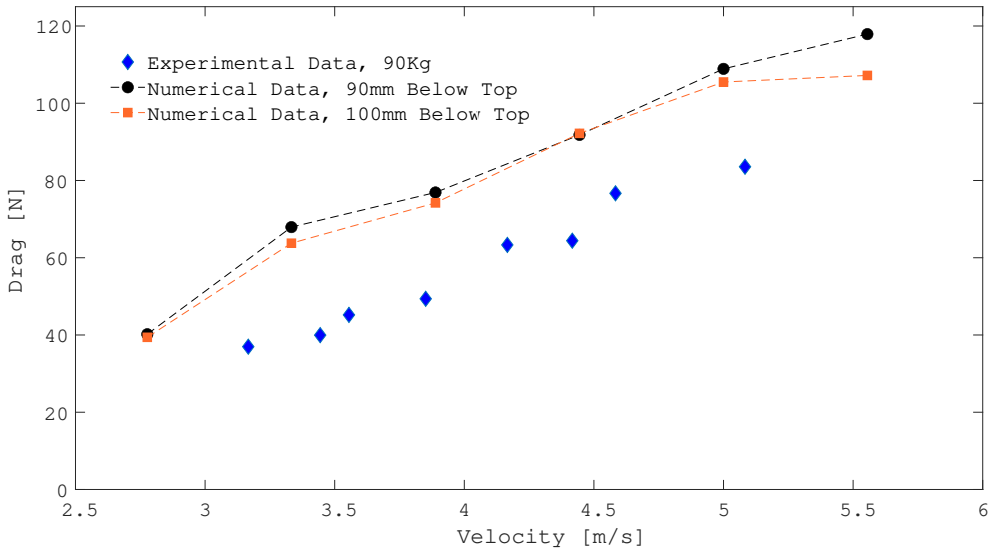

Figure 5.1: Total Resistance variation with velocity for C1 5 L.

These results are compared to the results obtained in the experimental tests made, for an athlete with $90\ kg$ of body mass. The waterline located $90\ mm$ below top corresponds to measured for the $90\ kg$ athlete in the field. The waterline located $100\ mm$ below top, corresponds to the measured for a $80\ kg$ athlete. The reason for simulating two waterlines is that

experimental tests were made for the weights corresponding to those same waterlines, and in order to directly compare the obtained results for both boats. Beside that, it is possible to compare the variation in results with a variation in the position of the waterline.

These results for C1 5 L do not have the intended accuracy when related to the experimental tests. This may be because the experimental tests have been done with a $90\ kg$ athlete, when the maximum recommended weight for the model L is $80\ kg$. Another possible factor was the measure of the waterline that has been done in the field, which leads us to some uncertainty in the obtained values. The waterline level used in the simulation was measured with the athlete at static rest. However, this value may not correspond to the moving value. Since the drag results are so sensible to the waterline value, due to the friction drag, directly affected by the wetted area, this value must be calculated accurately.

In this numerical model, open channel flow is used, and the waterline level is fixed at the domain inlet and outlet. Due to the approximation flow and the velocity of the flow at the inlet, it is difficult to guarantee the desire waterline value. After each iteration is difficult to ensure that the waterline position in the boat is the desired waterline measured in the field.

With a lower waterline, the numerical results seem to approximate the experimental results better, since both results growth trend to follow the tendency of the experimental results. Nevertheless, it can be seen that the $10\ mm$ difference in the water line only starts to have a significant difference in numerical results at higher velocities. These results are interesting to analyse, because an increase in muscle mass, and consequently an increase in the mass of the athlete, can be advantageous, due to the fact that it does not result in a significant increase in drag.

5.1.2 C1 8 L model

The drag variation with velocity results for the C1 8 L model is shown in Figure 5.2. In this graphic, there are also two waterlines, located $100\ mm$ below the top of the boat and another one located at $90\ mm$ below the top of the boat. These values were approximately those measured in the field, which $100\ mm$ below the top of the boat corresponds to the $80\ kg$ athlete and $90\ mm$ below top corresponds to a $90\ kg$ athlete.

These results are compared to the results obtained in experimental tests made for an athlete with $80\ kg$ body mass. In the case of C1 8 L, the numerical results are in good agreement with the experimental tests, relative to the previous model. In this test, the athlete body mass was around $80\ kg$, which is in the spectrum recommended by the manufactured. This could have influenced the results compared to tests for the other model. Therefore, it would be an advantage to realise the tests with the same athlete, even for comparison purposes. The drag appears to grow almost linearly with the increase of the velocity in this range. However, when compared to the C1 5 L model, it seems to have a less marked growth with the velocity increase. In relation to the position of the waterline, in this model, as in the previous, it is

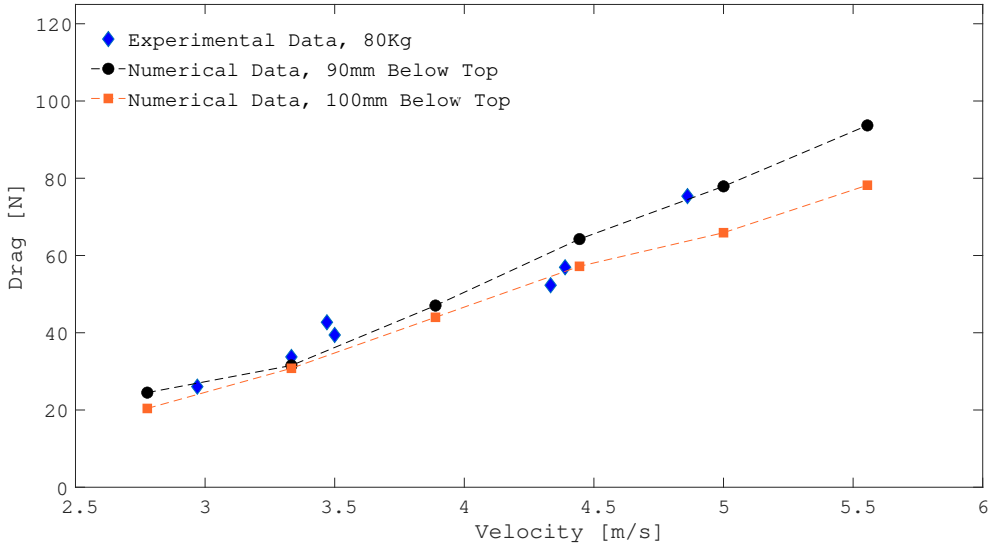

Figure 5.2: Total Resistance variation with speed for C1 8 L.

noted that the $10\ mm$ variation in the waterline position only starts to make a significant difference with the higher velocities.

5.2 C1 5 L vs C1 8 L

In this section, it will be compared both models. In this comparison, it will be used the constant velocity of $4.4\ m/s$ and constant waterline measured for an $80\ kg$ athlete. The choice of this velocity, is due to the fact that it is the average velocity of the top seats in a C1 $1000\ m$ Olympic event. On the other hand, the choice of the location of the waterline took into account the weight indications of the manufacturer, as well as the weight of the canoeing athletes using the models studied.

5.2.1 Velocity

Figures 5.3 and 5.4, represents the velocity contour for C1 5 L and C1 8 L, respectively, at a constant velocity of $4.4\ m/s$. These contours are relative to the waterline. They are relative to a plan created where the volume of fraction is equal to 0.5, in other words, at the interface between water and air.

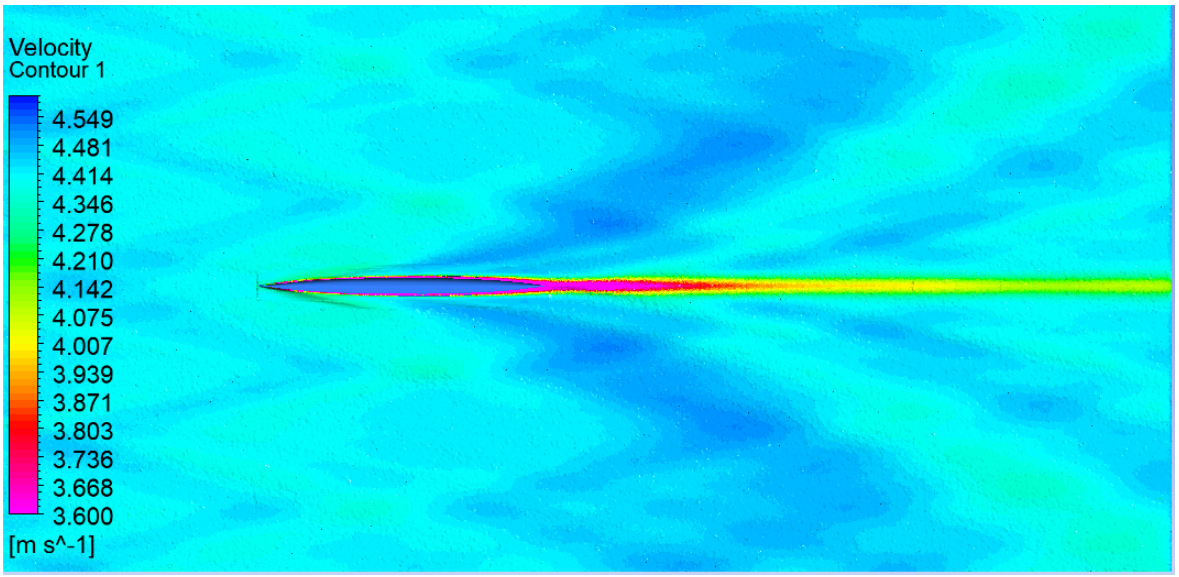

Figure 5.3: Waterline Velocity Contour at $4.44\ m/s$ for C1 5 L.

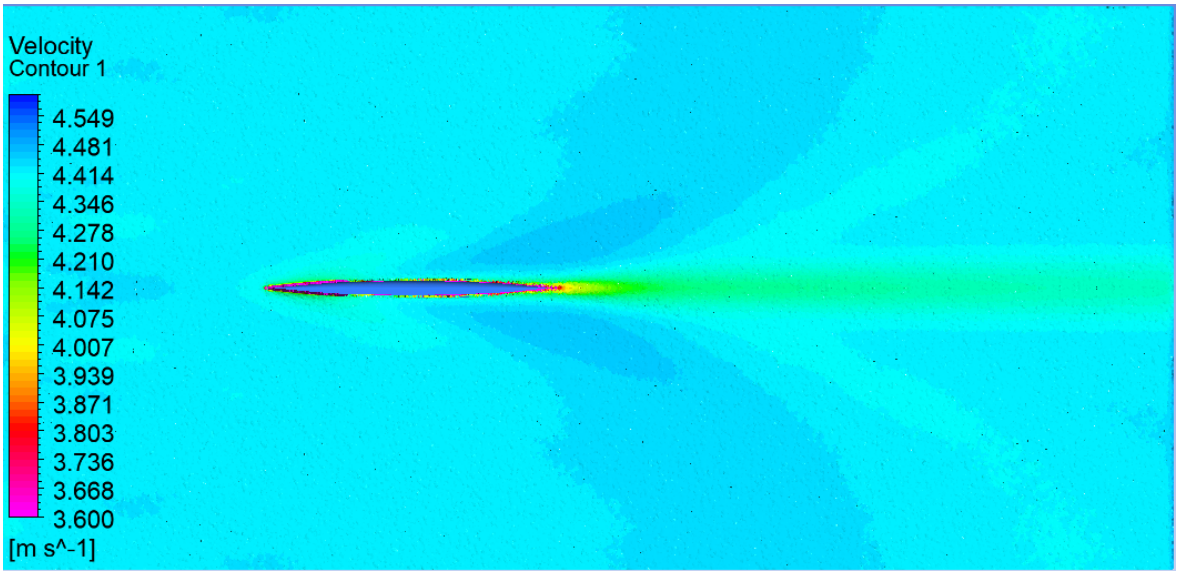

Figure 5.4: Waterline Velocity Contour at $4.44\ m/s$ for C1 8 L.

It is visible that there is a greater range of velocities in the case of C1 5 L. This variation of velocities in the figure is effect of increased drag, which is noticeable in the total drag results. In the wake of C1 5 L, a sharp decrease in velocity is noted when compared to C1 8 L. This low velocity in the wake of C1 5 L result from a greater friction drag when compared to C1 8 L and a greater wave elevation in the wake, as visible in Figure 5.5.

It is also visible, in the rear side of the canoe, an increase of velocity in boat canoes, most noted in C1 5 L. This increase of velocities is resultant from the wave trough, more visible in Subsection 5.2.2.

Noteworthy that in C1 5 L case, the velocity is not as stable as in C1 8 L case. However, these variations are resultant from some small waves, which have spread since the inlet, but are

considered irrelevant to the study because of their small size, when compared to the canoe dimensions.

5.2.2 Wave Elevation

Figures 5.5 and 5.6 represents the wave elevation for C1 5 L and C1 8 L, respectively, at a constant velocity of $4.4\ m/s$. To note that the figures have different scales, this is due to the fact that they have different geometries, which forced the reference in the domain to be different. In Figure 5.5 and Figure 5.7, the waterline level was set at Z=-0.24. In relation to Figure 5.6 and 5.8, the waterline level was set at Z=-0.29.

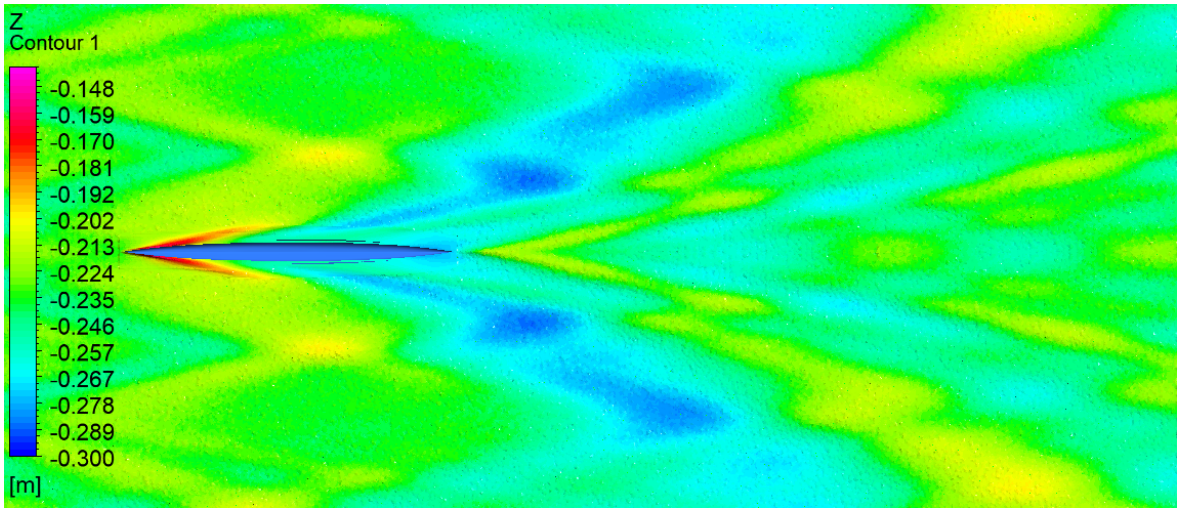

Figure 5.5: Wave Elevation at $4.44\ m/s$ for C1 5 L.

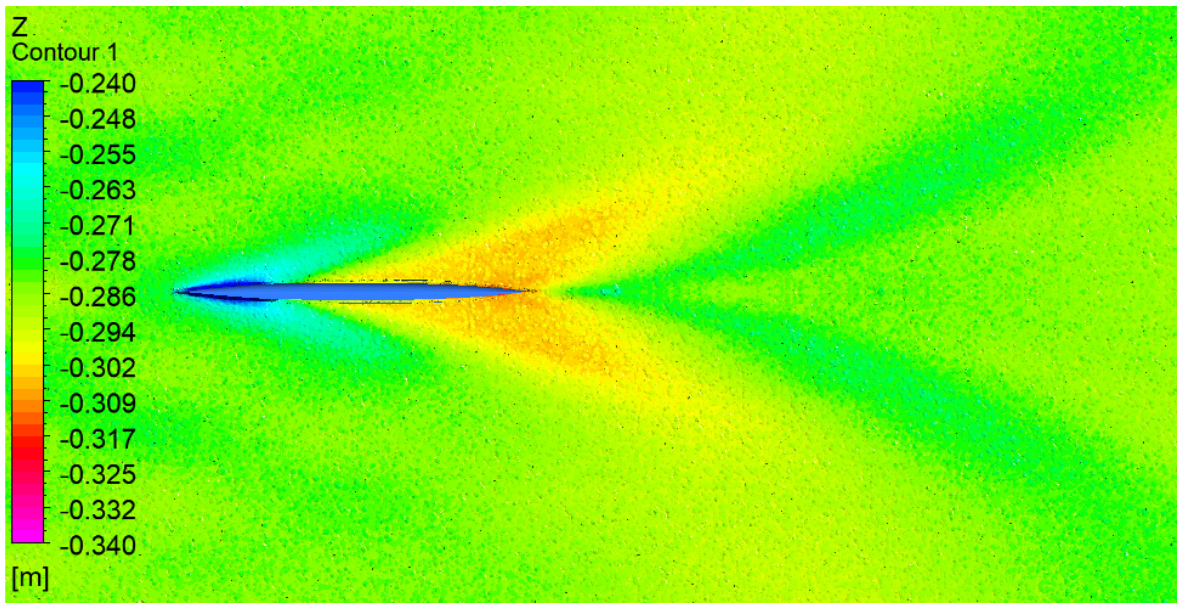

Figure 5.6: Wave Elevation at $4.44\ m/s$ for C1 8 L.

In Figure 5.5, it is visible the small waves mentioned in 5.2.1, in the upstream.

When compared both figures, it is noted that in C1 5 L case, the formation of larger waves is noted, and also, a formation of a relevant secondary wave. For the formation of these waves, energy is needed, which is being spent from the stroke of the athlete. Therefore, it can be concluded that C1 8 L spent less energy on wave formation when compared to C1 5 L.

It is also possible to note, in the C1 5 L case, a greater separation of the wave from the canoe. In the C1 8 L model, the wave follows the canoe line.

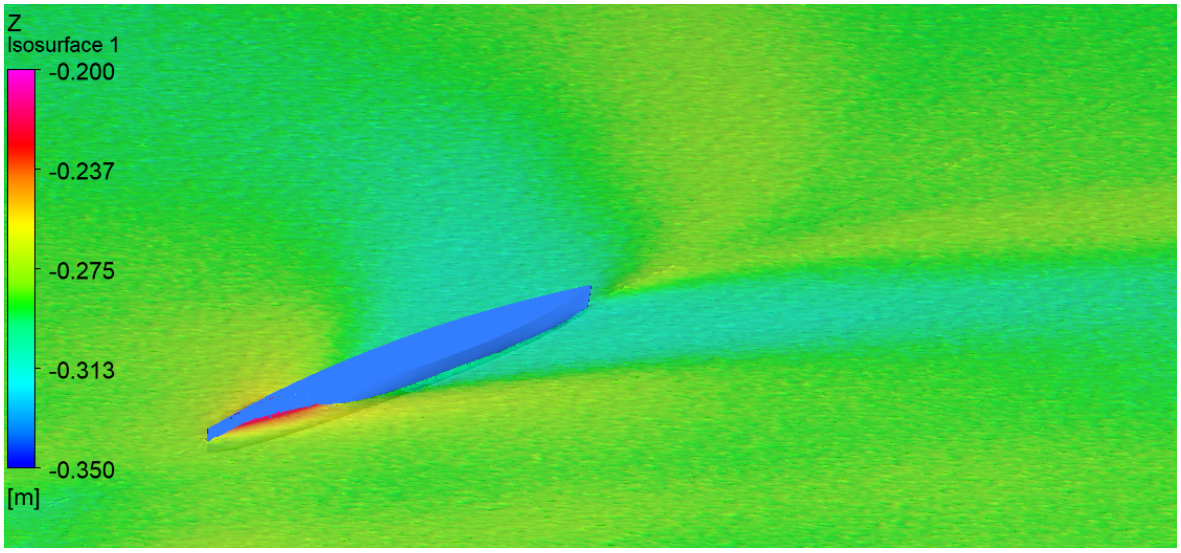

Figure 5.7: Wave Elevation in perspective at $4.44\ m/s$ for C1 5 L.

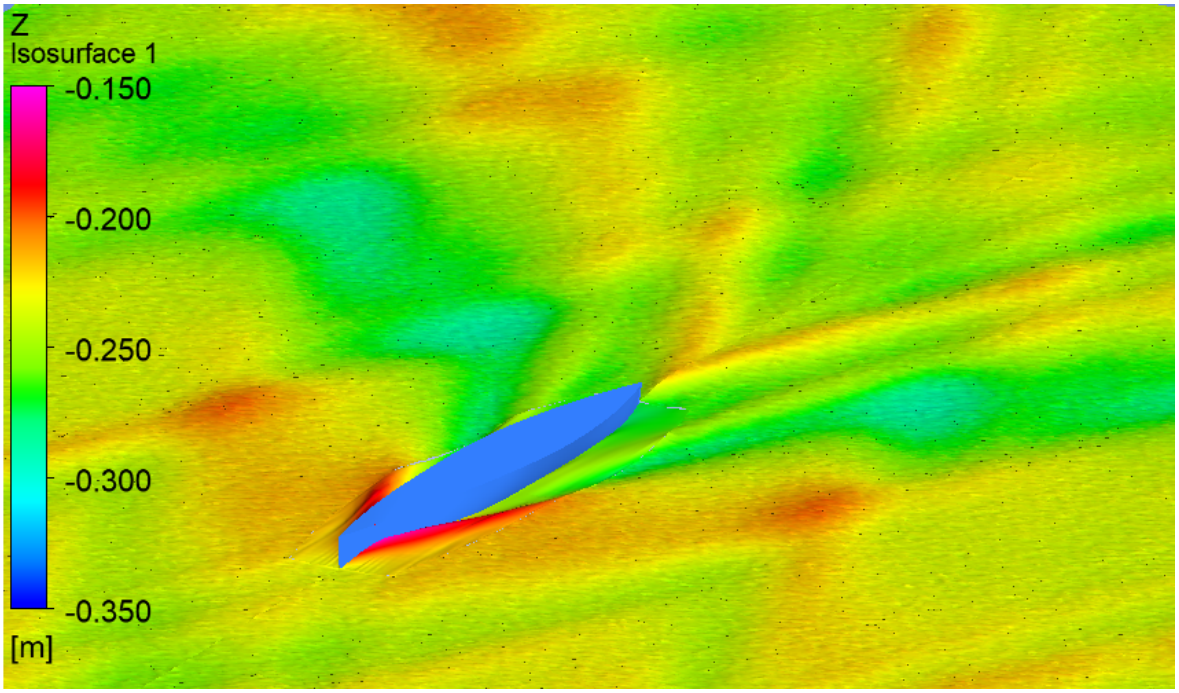

Figure 5.8: Wave Elevation in perspective at $4.44\ m/s$ for C1 8 L.

Figures 5.7 and 5.8 give a better view of the wave formation in both canoes. It is once again

noted, the bigger wave formation in the C1 5 L case and also the separation in the bow of the canoe.

5.2.3 Pitch Angle

During this dissertation, it was realised a study to evaluate the best position of the athlete in the boat. The centre of mass of the athlete will affect the pitch angle of the boat. A pulled forward centre of mass will translate into a negative pitch angle, with a bow sunk and a raised stern. On other hand, a centre of mass pulled behind will translate into a raised bow and a sunk stern. This variation will affect the performance of the boat.

In Figure 5.9, it is shown the drag values for different pitch angles. These angles vary between -0.5º and 0.5º since a greater range is impractical in reality.

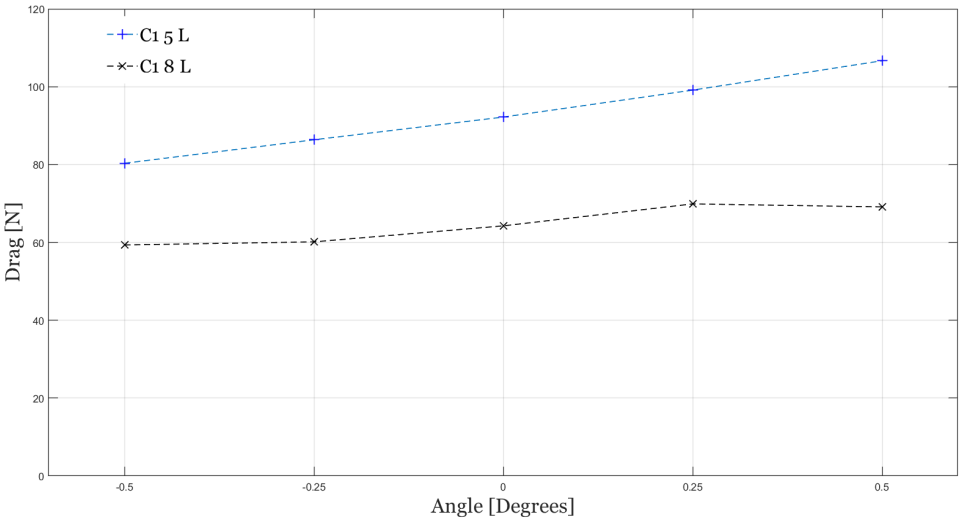

Figure 5.9: Total Resistance variation with pitch angle.

These values were calculated for a waterline measured for an $80\ kg$ athlete, with a constant velocity of $4.44\ m/s$ for both models.

As seen in Figure 5.9, is concluded that an athlete positioned further ahead on the boat may have improved performance. This change of position must take into account the comfort of the athlete during the paddle stroke, given that, the paddle movement itself oscillates the centre of mass longitudinally, in relation to the canoe.

This study was performed through a steady approach whereby, the hull is fixed in a point and the flow seeps around. This approach seems to be more correct for neutral positions, because in reality an athlete can not move with a constant attitude, negative or positive. In a real context, when rowing the athlete constantly varies his attitude, so this study aims only to study the behaviour of the boat with a constant pitch angle

Hereupon, it was interesting to compare these results with a transient study.

Chapter 6

Conclusions and Future Work

Finally, in this Chapter, it will be presented the conclusions reached in this work, and also some suggestion for future works are made.

6.1 Conclusions

In this dissertation, a numerical study has been developed, faced with the performed experimental tests. It was investigated the effects of the velocity and pitch angle on the drag of the boat using commercial software Ansys Fluent 2019 R3. It was used a steady approach, which seemed to be a good approximation for the real case for hull performance analysis.

The drag forces obtained for the C1 8 L are closer to the experimental results obtained when compared to the C1 5 L results. However, both seem to follow well the growth trend. The experimental results would be more conclusive if the test for both models had been done with the same $80\ kg$ athlete. It occurred some difficulties, such as the detailed prediction of the waterline position, that will affect the wetted area, crucial in the frictional drag component.

In relation to the pitch angle, it was concluded that an athlete with his centre of mass further on the boat, causing a negative pitch, may have advantages on the performance of the boat. Of course, the athlete will have more advantage paddling in a comfortable position where he can be stable and print more strength in each stroke, so these results are merely indicative. This study was also a steady approach where the hull remains in a fixed position, therefore, a transient study can bring more valid results in this section.

Given these results, it is concluded that the new model, C1 8 L has better performance when compared to the previous model, mainly due to the less formation of waves. These results show that, at this Froude number scale, the wave drag starts to become more evident.

6.2 Future Work

After finished this work, some future works are suggested, as well as possible indications that could help in these works.

In this study, it was numerically simulated a steady approach of this case, which proved to be a good approximation in most cases, however, in future works, a transient study may be

performed for a better flow simulation, and comparison with this work, especially to simulate the paddling stroke.

Another conclusion reached was related to the roughness of the boat. In this study, it is assumed that both boats have the same value for this property, which may not be correct and affect the results. In future works, is interesting to predict these values for both canoes and study the optimal coating for the boat hull.

It is also suggested for future works to study the influence of the paddle stroke in the hull flow, to optimise the drag values. It is also interesting to study the design of the paddle blade since in the boat design, the construction rules are more restrictive while in the paddle blade design the rules are not so much. So, it can be more advantageous to change the blade design than the hull design, to obtain better results.

Bibliography

[1] Infopédia, "Ciência Náutica Portuguesa - Infopédia." [Online]. Available: https://www.infopedia.pt/$ciencia-nautica-portuguesa

[2] N. Warzecha, "Germany Rocks on Water." [Online]. Available: https://www.ansys.com/ko-kr/resource-library/article/germany-rocks-on-water-ansys-advantage-v6-i2

[3] "History," Aug. 2015. [Online]. Available: https://www.canoeicf.com/history

[4] "Canoe Sprint," Jul. 2015. [Online]. Available: https://www.canoeicf.com/disciplines/canoe-sprint

[5] "Canoe Slalom," Jul. 2015. [Online]. Available: https://www.canoeicf.com/disciplines/canoe-slalom

[6] "Rules," Aug. 2015. [Online]. Available: https://www.canoeicf.com/rules

[7] T. J. Bugalski, "Hydromechanics for development of sprint canoes for the olympic games," *Plastex: high performances print boats and paddles.–Gdansk, Poland*, 2010.

[8] M. G. Robinson, L. E. Holt, and T. W. Pelham, "The technology of sprint racing canoe and kayak hull and paddle designs," *International Sports Journal*, vol. 6, no. 2, pp. 68–85, 2002.

[9] J. S. Michael, R. Smith, and K. B. Rooney, "Determinants of kayak paddling performance," *Sports Biomechanics*, vol. 8, no. 2, pp. 167–179, 2009.

[10] A. Molland, S. Turnock, and D. Hudson, "Components of hull resistance," *Ship Resistance and Propulsion: Practical Estimation of Propulsive Power. Cambridge University Press, Cambridge*, pp. 12–68, 2011.

[11] "Boat Hull Types, Designs & Explanations." [Online]. Available: https://www.boaterexam.com/boating-resources/boat-hull-types-designs.aspx

[12] C. Danielson, *Displacement Hull Catamaran Letter of Transmittal*, Florida, 2006.

[13] D. Pendergast, D. Bushnell, D. Wilson, and P. Cerretelli, "Energetics of kayaking," *European journal of applied physiology and occupational physiology*, vol. 59, no. 5, pp. 342–350, 1989.

[14] P. Jackson, "Performance prediction for olympic kayaks," *Journal of sports Sciences*,

vol. 13, no. 3, pp. 239–245, 1995.

[15] J. N. Newman, *Marine hydrodynamics*. The MIT press, 2018.

[16] B. Lee, C. Lee, Y. Kim, and K. Ko, "Prediction of ship wave crests on varying water depths and verification by flow-3d," *Journal of The Korean Society of Civil Engineers*, vol. 33, 07 2013.

[17] H. O. Kristensen and M. Lützen, "Prediction of resistance and propulsion power of ships," *Clean Shipping Currents*, vol. 1, no. 6, pp. 1–52, 2012.

[18] Y. M. Ahmed, "Numerical simulation for the free surface flow around a complex ship hull form at different froude numbers," *Alexandria Engineering Journal*, vol. 50, no. 3, pp. 229–235, 2011.

[19] L. Larsson and L. Broberg, "A method for resistance and flow prediction in ship design," 1990.

[20] B. B. Gomes, L. Machado, N. V. Ramos, F. A. Conceição, R. H. Sanders, M. A. Vaz, J. P. Vilas-Boas, and D. R. Pendergast, "Effect of wetted surface area on friction, pressure, wave and total drag of a kayak," *Sports biomechanics*, vol. 17, no. 4, pp. 453–461, 2018.

[21] L. Formaggia, E. Miglio, A. Mola, and A. Montano, "A model for the dynamics of rowing boats," *International journal for numerical methods in fluids*, vol. 61, no. 2, pp. 119–143, 2009.

[22] R. K. Hanna, "Cfd in sport-a retrospective; 1992-2012," *Procedia Engineering*, vol. 34, pp. 622–627, 2012.

[23] A. Bible, "Canoe hull technology," *Paddler*, vol. 18, no. 2, p. 18, 1998.

[24] G. D. Tzabiras, S. P. Polyzos, K. Sfakianaki, V. Diafas, A. D. Villiotis, K. Chrisikopoulos, and S. Kaloupsis, "Experimental and numerical study of the flow past the olympic class k-1 flat water racing kayak at steady speed," *The Sport Journal*, vol. 13, pp. 1–15, 2010.

[25] B. B. Gomes, F. A. Conceição, D. R. Pendergast, R. H. Sanders, M. A. Vaz, and J. P. Vilas-Boas, "Is passive drag dependent on the interaction of kayak design and paddler weight in flat-water kayaking?" *Sports Biomechanics*, vol. 14, no. 4, pp. 394–403, 2015.

[26] Y.-T. Oh, B. Burkett, C. Osborough, D. Formosa, and C. Payton, "London 2012 paralympic swimming: passive drag and the classification system," *British journal of sports medicine*, vol. 47, no. 13, pp. 838–843, 2013.

[27] A. Fluent, "Ansys fluent theory guide 15.0," *ANSYS, Canonsburg, PA*, vol. 33, 2013.

[28] V. d. Brederode, “Fundamentos de aerodinâmica incompressível,” *Edição do autor*, 1997.

[29] V. R. Mantha, A. J. Silva, D. A. Marinho, and A. I. Rouboa, “Numerical simulation of two-phase flow around flatwater competition kayak design-evolution models,” *Journal of applied biomechanics*, vol. 29, no. 3, pp. 270–278, 2013.

[30] J. Matsson, *An Introduction to ANSYS Fluent 2019*. SDC Publications, 2020.

[31] N. Warzecha and A. Spille-Kohoff, “Going for the gold,” *ADVANTAGE*, p. 20, 2007.

[32] F. L. da Rocha Barros, *”Study of Kayak Hull Design on Calm Water Resistance”*. FEUP, 2015.

[33] D. Morgoch, C. Galipeau, and S. Tullis, “Sprint canoe blade hydrodynamics-modeling and on-water measurement,” *Procedia engineering*, vol. 147, pp. 299–304, 2016.

[34] A. Leroyer, J. Wackers, P. Queutey, and E. Guilmineau, “Numerical strategies to speed up cfd computations with free surface—application to the dynamic equilibrium of hulls,” *Ocean engineering*, vol. 38, no. 17-18, pp. 2070–2076, 2011.